RSC Mechanochemistry

ROYAL SOCIETY OF CHEMISTRY

REVIEW

View Article Online
View Journal

Cite this: DOI: 10.1039/d5mr00116a

Force-driven architectonics of inorganic nanomaterials: pathways to smart and functional interfaces

Mohammed Ali Dheyab, *[ab] Wesam Abdullah, [a] Sara Abdulwahab, [a] Sadeen Metib Alsarayreh, [a] Mothana Hussein Tarawneh, [a] Mutaz Mohammad Alsardi, [a] Mansour A. Alanazi [c] and Azlan Abdul Aziz[ab]

The deliberate structuring of inorganic nanomaterials through mechanical forces offers a powerful alternative to conventional synthesis, enabling solvent-free, energy-efficient, and scalable design strategies. Rather than serving only as a synthetic shortcut, force-driven processing is increasingly recognized as an architectonic tool as a means of directing matter into well-defined architectures that integrate top-down shaping with bottom-up assembly. This review develops a conceptual framework of architectonics under mechanical activation, treating external force as a design parameter that dictates structure formation across multiple length scales. Methodological platforms such as ball milling, extrusion, and hybrid force–stimuli systems are systematically assessed, alongside mechanistic insights spanning multiscale reaction pathways, computational modeling, and AI-enabled predictions. The potential of this approach to generate smart and functional interfaces is highlighted through applications in catalytic and energy conversion processes, biomedical nanomedicine, and electronic or sensing devices. Finally, we discuss current limitations particularly gaps in mechanistic understanding, predictive control, and scalability and outline future opportunities to advance force-driven architectonics as a foundation for next-generation functional inorganic nanomaterials.

Received 10th September 2025
Accepted 3rd January 2026

DOI: 10.1039/d5mr00116a

rsc.li/RSCMechanochem

1. Introduction

Mechanochemistry, as defined by the International Union of Pure and Applied Chemistry (IUPAC) Compendium of Chemical Terminology, refers to chemical reactions induced by mechanical energy,[1] while Heinicke further described it as encompassing chemical and physico-chemical transformations of substances in all states of aggregation under mechanical force.[2] Building on this foundation, Takacs *et al.*[3] demonstrated that mechanical force produces qualitatively distinct outcomes compared to thermal or photochemical treatments, establishing an early cornerstone for the field. Over recent decades, mechanochemistry has evolved from a scientific curiosity into a versatile methodology enabling solvent-free, reproducible, and scalable transformations aligned with the principles of green chemistry.[4–6]

Ball milling in particular has re-emerged as a powerful solid-state technique, providing the necessary mechanical energy to drive reactions rapidly and under environmentally benign conditions.[7,8] Initially considered a top-down comminution process for producing micro- and nanoscale powders,[2,9] milling is now innovatively adapted for bottom-up nanoparticle synthesis through chemical reactions.[10,11] Mechanochemical grinding of oxides exemplifies this dual role, where simultaneous physical and chemical processes occur in coordinated patterns, yielding superior fine powders compared to conventional routes.[8,12] Despite its simplicity, mechanical milling often induces amorphization and surface defects, as shown by Šepelak's observation of 2–5 nm amorphous surface layers on oxide nanoparticles,[13,14] yet these very features underpin the phenomenon of mechanical activation. More broadly, mechanochemical approaches such as mechanical milling, alloying, reactive extrusion, and induced solid-state reactions offer efficient, solvent-free, and sustainable routes for producing nanocrystalline materials and functional composites.[15–17] Recognized as a pillar of green chemistry, mechanochemistry has been named by IUPAC among the top ten chemical innovations shaping sustainable science,[18] underscoring its relevance for modern material design. Compared with conventional wet-chemistry syntheses that generate solvent waste, involve prolonged treatment times, and require multistep drying or

[a]School of Physics, Universiti Sains Malaysia, 11800 Pulau Pinang, Malaysia. E-mail: mdali@usm.my; lan@usm.my

[b]Nano-Biotechnology Research and Innovation (NanoBRI), Institute for Research in Molecular Medicine (INFORMM), Universiti Sains Malaysia, 11800, Pulau Pinang, Malaysia

[c]Department of Physics, College of Science, Northern Border University, Arar P. O. Box 1321, Saudi Arabia

surfactant-assisted procedures,[8,19,20] mechanosynthesis bypasses solubility limitations and reduces hazardous waste while lowering energy input and reaction time.[21–24] These advantages have enabled the scalable, solvent-free synthesis of diverse nanomaterials, including oxides (TiO_2, CeO_2, Gd_2O_3) and metals such as Fe,[25] as well as perovskites, catalytic systems, and superhydrophobic surfaces.[15,16,20,26]

In recent years, applications of mechanochemical synthesis have expanded into pharmaceuticals, ligand design, drug synthesis, graphene production, and the surface modification of nanomaterials.[23,27] Importantly, soft mechanochemical strategies employing solid acids, bases, hydrated compounds, or salts have opened new opportunities for tailoring inorganic nanostructures,[28] while dry synthesis routes minimize solvents or surfactants, providing significant ecological and functional benefits.[29–32] The performance of noble metal nanoparticles, governed by size, shape, composition, and elemental distribution, further illustrates the critical role of mechanochemistry in advancing functional nanomaterials, as their catalytic, electronic, optical, and biomedical properties extend far beyond the aesthetic appeal that first inspired their study.[33,34] Collectively, these advances position mechanochemistry as a transformative platform for nanomaterials synthesis, bridging multiscale pathways of activation and assembly with the design of smart and functional interfaces.

Nonetheless, despite these achievements, previous academic research on mechanochemical synthesis has primarily emphasized scalability, solvent-free operation, and sustainability benefits, while leaving critical gaps unaddressed. Notably, Fiss *et al.*[35] highlighted the advantages of mechanochemical strategies in inorganic redox and ion-exchange processes, yet their analysis lacks mechanistic depth and broader sustainability

Mohammed Ali Dheyab

Dr Mohammed Ali Dheyab is a Lecturer at the School of Physics, Universiti Sains Malaysia (USM), and leads research at NanoBRI@INFORMM. He is a distinguished early-career researcher, recognized among Stanford University's "World's Top 2%" scientists for three consecutive years (2022–2025). His expertise lies in the green synthesis and biomedical applications of nanoparticles, with a focus on sustainable nanotechnology for medical and environmental innovations. Dr Dheyab completed his PhD in Physics in 2021 at Universiti Sains Malaysia, specializing in nanotechnology for medical applications. His research portfolio includes green-synthesized metal and metal oxide nanoparticles for cancer therapy, photothermal therapy, diagnostic imaging, and biocatalysis. He has an h*-index of 37 (Google Scholar) and is committed to mentoring students, advocating for environmentally friendly methodologies in nanomaterial synthesis for cancer treatment.*

Wesam Abdullah

Wesam Abdullah is a PhD researcher at Universiti Sains Malaysia (USM), where her work focuses on the development of advanced green nanomaterials including gold, silver, and iron oxide nanoparticles, as well as nanozymes for biomedical and radiation-related applications. Her research integrates nanotechnology with medical physics to advance diagnostic precision and therapeutic efficiency. She has published her work in several high-impact international journals.

Sara Abdulwahab

Sara Abdulwahab is pursuing her PhD at Universiti Sains Malaysia (USM), focusing on the development of functional green nanoemulsions for biomedical and environmental applications. Her research emphasizes sustainable synthesis and surface engineering strategies to enhance stability and targeted delivery performance.

Sadeen Metib Alsarayreh

Sadeen Metib Alsarayreh is pursuing her PhD at Universiti Sains Malaysia (USM), focusing on the synthesis and functional engineering of manganese dioxide (MnO_2)-based nanomaterials for biomedical applications. Her research emphasizes controlled fabrication, surface modification, and redox-responsive design strategies to enhance stability, catalytic performance, and targeted biomedical functionality.

metrics beyond nanoparticles and hybrid frameworks such as metal–organic frameworks (MOFs). While MOFs are classified as organic–inorganic hybrid systems, their inclusion in mechanochemical discussions is common due to their highly crystalline architectures and force-responsive porosity, which often parallel the behaviors of inorganic nanomaterials. Likewise, Auvray and Friščić[6] offered valuable mechanistic insights and a systematic classification for hard and high-melting inorganic materials, but their work overlooks opportunities in nanomedicine and hybrid nanostructures. Similarly, Xu *et al.*[16] underscored the simplicity and catalytic benefits of mechanochemical synthesis as a green alternative to conventional routes, although their discussion remains confined to catalysis, neglecting wider applications in energy storage and biomedical interfaces. In light of these deficiencies, our review aims to address the unmet need for a cross-disciplinary framework in mechanochemical synthesis of inorganic nanomaterials. We provide a coherent architectonic perspective that goes beyond catalysis and selected inorganic systems, integrating methodological platforms, mechanistic insights, and smart interface engineering. By systematically linking force-driven design to functional outcomes in catalysis, energy storage, and biomedicine, we establish mechanochemistry as a versatile architectonic tool rather than a niche synthetic route. This exclusive focus on designing smart and functional interfaces aligns with global priorities for sustainable, scalable, and multifunctional nanomaterials, offering a roadmap for future advances across chemistry, materials science, and nanomedicine.

Mothana Hussein Tarawneh

Mothana Hussein Tarawneh is a PhD candidate at Universiti Sains Malaysia (USM), where his research centers on MXene-derived nanostructures for diagnostic imaging and radiation-based applications. His work integrates material science with radiation physics to advance multifunctional theranostic platforms.

Mutaz Mohammad Alsardi

Mutaz Mohammad Alsardi is a PhD researcher at Universiti Sains Malaysia (USM), specializing in MXene-based nanomaterials for advanced radiotherapy and imaging. His study bridges nanotechnology and medical physics, targeting enhanced radiation sensitivity and precision in cancer treatment.

2. Mechanochemical architectonics: conceptual framework

2.1. Defining "architectonics" in mechanochemistry

Mechanochemical architectonics reframes the synthesis of inorganic nanomaterials as a deliberate, multiscale strategy that couples mechanical energy input with interfacial design principles to yield functional architectures rather than merely discrete particles. In this framework, architectonics denotes the purposeful construction of structure function relationships across length scales ranging from atomic arrangements and defect structures to particle morphology and interfacial connectivity. Mechanical actions such as impact, shear, or extrusion serve as orthogonal variables that control crystallinity, defect chemistry, surface coordination, and assembly pathways. Unlike conventional thermal or solution-based routes, mechanochemical reactions (i) activate otherwise inaccessible transformations by generating high-energy defect states and transient solid–solid contacts, (ii) impose nonequilibrium mixing that favors metastable polymorphs or alloying, and (iii) induce tribochemical processes that produce unique interfacial chemistries. These attributes establish mechanochemistry as a versatile lever for architectonic control.[36,37]

The power of mechanochemical architectonics comes from three interconnected processes (Fig. 1). First, the intense local stresses and collisions during milling distort the crystal lattice and create defect-rich areas. These defects make it easier for ions to move and redox reactions to happen, allowing solids like metals and oxides to transform quickly at the atomic level.[38] For instance, when making metal oxide nanoparticles like Fe_2O_3, milling causes repeated breaking and welding of particles, which increases defects and speeds up reactions that would normally require high heat, enabling them to occur near room temperature.[39] Second, the constant cycle of cold welding and fracturing during milling keeps generating fresh, reactive surfaces and dynamic interfaces between solids. These tiny

Azlan Abdul Aziz

Prof. Dr Azlan Abdul Aziz is a Professor of Nanomaterials and Nanostructures at the School of Physics, Universiti Sains Malaysia (USM). He received his MSc in Microelectronics Material and Device Technology in 1994 and completed his PhD in 1999 at the University of Manchester Institute of Science and Technology, specializing in high electron mobility transistors (HEMT) grown by molecular beam epitaxy. He leads research at NanoLAB and NanoBRI@INFORMM, focusing on nanostructured materials for sensor applications, ZnO- and GaN-based materials for gas and light sensing, and III–V device simulations. With >6700 citations and an h*-index of 46 (Google Scholar), he has significantly advanced solid-state physics and nanotechnology research.*

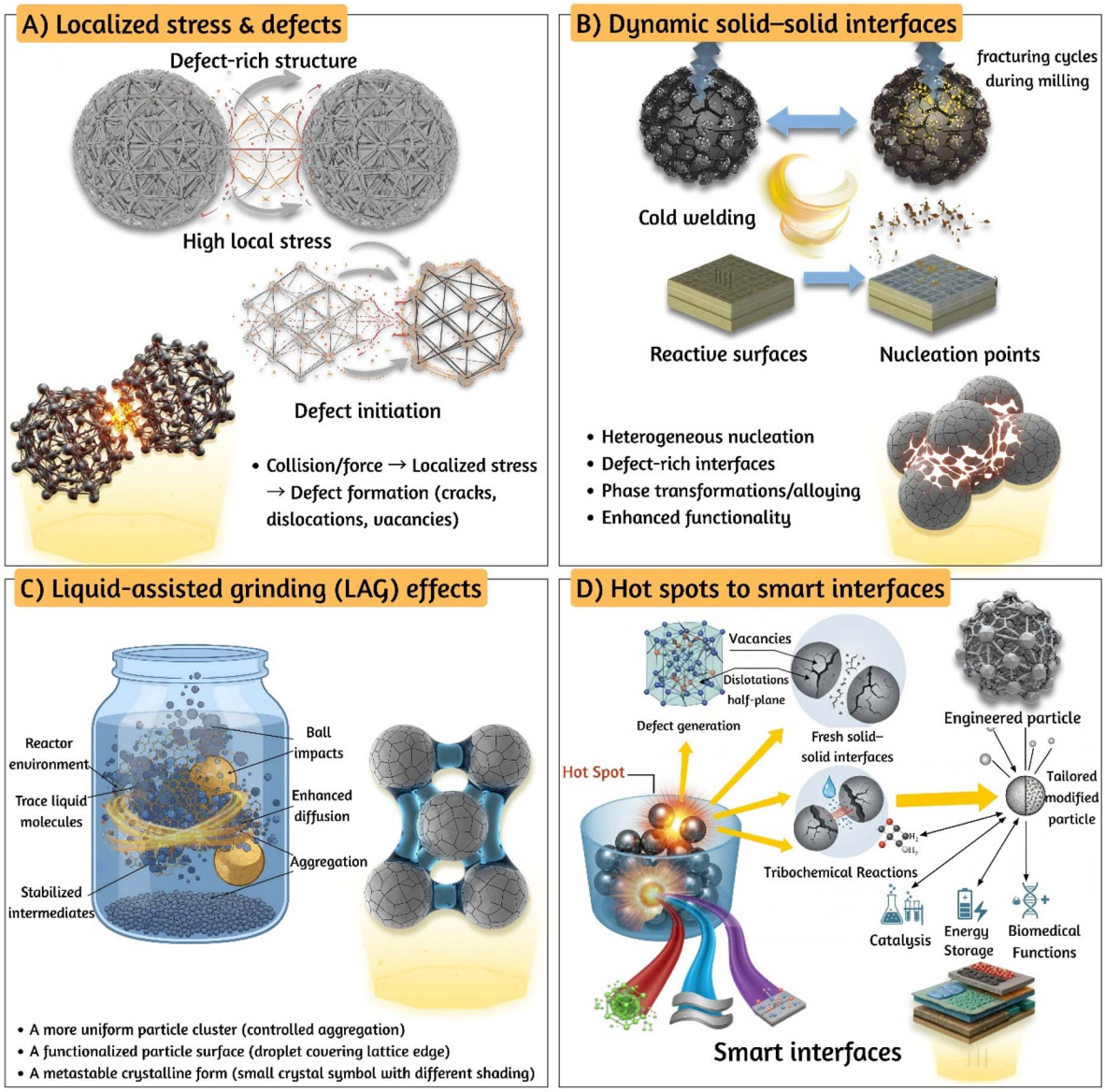

Fig. 1 Mechanochemical architectonics illustrated through four key processes: (A) localized stress and defect generation induce lattice distortions that lower activation barriers; (B) dynamic solid–solid interfaces formed by cyclic cold welding and fracturing regenerate reactive surfaces controlling morphology; (C) liquid-assisted grinding introduces small liquid films that modulate capillary and solvation forces to guide particle assembly; (D) particle collisions generate localized 'hot spots' that drive defect formation, transient intermediates, and fresh interfaces. These dynamic pathways converge to create 'smart interfaces' with controlled structure and chemistry, enabling enhanced catalytic, energy, and optical functions.

surfaces act like small reactors where the chemistry occurs how many of these nucleation spots form and their chemical nature ultimately shape the final product. A good example is making mixed oxides like titanium dioxide (TiO_2) and cerium dioxide (CeO_2) by milling: the process disperses these oxides evenly and mixes them at the nanoscale, resulting in catalysts with unique properties without needing to heat them in bulk.[40] Mechanochemical milling of TiO_2–CeO_2 at 350 rpm for 100 min yields nanoscale composites with particle sizes ~5 μm and enhanced oxygen sensitivity (up to 8.2 at 320 °C), demonstrating force-driven architectonics without bulk heating. Third, adding small amounts of liquid during milling (called liquid-assisted grinding) changes how energy moves and how surfaces interact. This helps guide how particles aggregate or bond on the surface, offering precise control over the assembly and functionalization of particles.[38] This combination of mechanical stress, dynamic surface creation, and liquid effects makes mechanochemical architectonics a powerful method for designing and synthesizing advanced materials efficiently and in environmentally friendly ways.

Shi *et al.*[41] demonstrate a form of nano architectonics by embedding Pt single-atoms and differently-sized Pt nanoparticles (1.5, 3.0, and 7.0 nm) onto manganese-oxide nanosheets. Although the synthesis was not purely mechanochemical, the principles of architectonics namely, vacancy filling, atomic dispersion, and interface-driven functionality are central to the

material's catalytic behavior. The manganese-oxide nanosheets serve as a defect-rich scaffold, with oxygen vacancies acting as anchoring sites for Pt species. The interaction between Pt and MnO_2 is not merely compositional but architectonic: it alters the oxidation state of manganese, modulates the oxygen vacancy concentration, and tunes the catalytic activity of the hybrid nanozyme. This reflects the essence of mechanochemical architectonics where structure and function co-evolve through controlled energy input and spatial design.

Despite its promise, several limitations constrain the broader adoption of mechanochemical architectonics. Reproducibility and parameter standardization remain persistent challenges: milling frequency, ball-to-powder ratio, filling factor, and jar geometry introduce nonlinear effects on energy input and product distribution, complicating cross-study comparisons. Contamination from milling media, together with uncontrolled localized heating, may obscure mechanistic interpretation and compromise functional performance. Scale-up is particularly problematic, as laboratory-scale ball mills generate heterogeneous energy distributions that are not easily replicated in continuous or industrial platforms. Furthermore, mechanistic insights are often inferred from *ex situ* characterizations, which risk conflating transient intermediates with end products.[42]

Several strategies have been proposed to address these limitations and strengthen the mechanochemical toolkit. Standardized reporting of energy metrics (*e.g.*, J g^{-1} or specific impact energy) would enable quantitative comparison across studies. Media wear and contamination can be minimized through careful selection of ceramic liners and inert milling components. The systematic use of Liquid-Assisted Grinding (LAG), rather than as an ad hoc additive, allows controlled tuning of interfacial chemistry. Hybrid activation methods combining mechanical milling with thermal annealing, sonication, or photonic inputs may further decouple defect generation from morphological evolution. Most critically, real-time monitoring through acoustic emission, synchrotron X-ray scattering, Raman spectroscopy, and *operando* temperature–pressure probes offer the potential to resolve transient intermediates and establish direct correlations between energy input and physicochemical outcomes. The development of scalable, continuous mechanochemical reactors such as twin-screw extruders and reactive ion-milling devices, validated against batch systems with conserved energy metrics, represents an essential step toward industrial translation.[43]

A central mechanistic underpinning is the generation of localized, transient high-energy sites commonly referred to as "hot spots" which store strain energy and enable bond cleavage and atomic rearrangements without the need for bulk thermal activation.[44] The stochastic nature of collisions and nonequilibrium energy distributions during milling open pathways inaccessible to conventional methods, resulting in accelerated reaction rates, selective product formation, and stabilization of otherwise unstable intermediates. This capacity to create dynamically evolving "smart" interfaces, where chemical state, morphology, and function are continuously reconfigured under mechanical stress, provides a rational basis for enhanced catalytic, electronic, and optical performance.[45]

Recent studies illustrate these dynamics with increasing clarity. For instance, the mechanochemical synthesis of MOFs such as MOF-74 proceeds through rapid formation of short-lived intermediates, with liquid additives accelerating coordination and structural reorganization. *In situ* powder X-ray diffraction (PXRD) has revealed that these intermediates adopt distinct coordination motifs or polymorphic forms, highlighting the structural dynamism inherent to mechanochemical pathways.[46] Klimakow *et al.*[47] highlight mechanochemical architectonics is exemplified through the solvent-free synthesis of MOFs, specifically HKUST-1 and MOF-14, using ball milling techniques. The authors demonstrate that mechanical energy can be harnessed not only to drive chemical reactions but also to sculpt the pore architecture and surface properties of the resulting materials. This approach yields high specific surface areas up to 1713 $m^2\ g^{-1}$ comparable to the best values reported *via* conventional solvothermal methods, yet achieved without solvents or extensive post-synthetic treatments. Similarly, mechanochemical anion-exchange in lead(II) coordination polymers demonstrates crystal-to-crystal transformations that preserve crystallinity while enabling functional modulation, underscoring the potential of architectonics to deliver solvent-minimized, highly efficient material design strategies.[48]

The objectives of architectonics are realized by intentionally guiding how simple molecular or nanoscale units organize into more complex and functional architectures. Rather than relying on spontaneous assembly, architectonic design emphasizes control over interfacial interactions, defect formation, and assembly pathways, allowing structure to evolve in a predictable manner across length scales. In mechanochemical systems, mechanical force serves not only as an energy source but also as a regulating element that influences contact dynamics, surface reactivity, and kinetic pathways. Through careful adjustment of processing conditions and chemical environments, this approach enables a direct connection between architectural design and material performance.[49,50] This architectonic perspective provides the foundation for treating mechanical force not merely as an energy source, but as a tunable design parameter.

2.2. Force as a design parameter

Mechanochemical force is not simply an energetic input it is a tunable design parameter, finely controllable and capable of directing reaction pathways, structural outcomes, and interfacial functionality. In contrast to thermal or solution-based methods, mechanical force in milling is discrete, spatially heterogeneous, and temporally dynamic, offering unparalleled opportunity for architectonic control.[51] At the microscopic level, force defines the nature and density of reactive sites. Higher milling frequencies and greater impact energies induce localized lattice distortions, shear bands, and defect clusters that dramatically reduce activation barriers for ionic migration or redox transformations. For example, increasing frequency from 15 to 30 Hz in a ball mill amplifies single-collision energies nearly fourfold (0.49 mJ to 1.96 mJ), translating directly into faster conversions in C–C coupling reactions and enhanced

solid-state diffusion in alloy formation. Here, single collision energy refers to the mechanical energy transferred during an individual impact event between the milling media and the material. The energy values reported in mJ correspond to milli-Joules (10^{-3} J).[52] This correlation underscores why force tuning enables mechanochemical pathways inaccessible to conventional routes: the creation of transient, high-energy states that bias metastable phase formation, alloying, or selective bond scission. To consolidate force as a mechanistic design variable, Fig. 2 couples applied mechanical input with experimentally validated structural evolution pathways in mechanochemical systems. Increasing collision energy and frequency drive force-dependent transitions from lattice distortion and defect nucleation to metastable intermediate formation, amorphization, or selective recrystallization, as directly observed by *in situ* synchrotron PXRD through time-resolved changes in phase fraction and peak broadening.[53] Complementary *operando* Raman spectroscopy captures force-induced bond reorganization and intermediate lifetimes, confirming that mechanical force reshapes reaction energy landscapes rather than merely accelerating kinetics. The figure further highlights intrinsic force heterogeneity, where localized high-energy "hot spots" coexist with under-energized regions, providing a physical basis for simultaneous crystalline, amorphous, and defect-rich domains within a single milling environment.[51]

Additionally, force controls how solid–solid interactions collectively evolve. The balance between fracturing and cold welding, controlled by milling intensity and ball-to-powder ratio (BPR), regulates the frequency of interface renewal and the density of nucleation sites. High BPRs accelerate composite synthesis, as demonstrated in molybdenum disilicide ($MoSi_2$) and titanium carbide (TiC) systems where a 20 : 1 ratio completed conversion in 10 h compared to incomplete reaction at 5 : 1 even after 30 h.[54] Similarly, denser milling media such as zirconium dioxide (ZrO_2) or tungsten carbide (WC) deliver sharper impacts that promote rapid defect generation but can also over-fragment sensitive phases, producing amorphization or unintended contaminations.[54] These trade-offs illustrate the duality of force: it can either enable rapid architectonic assembly or induce destructive over-milling.

Despite its centrality, quantitative control of force in mechanochemical synthesis remains underdeveloped. Most studies report milling parameters such as frequency, ball size, or jar material but these serve as indirect proxies rather than true measures of force. Without standardized reporting of impact energy (J g^{-1}), collision frequency, or energy density,

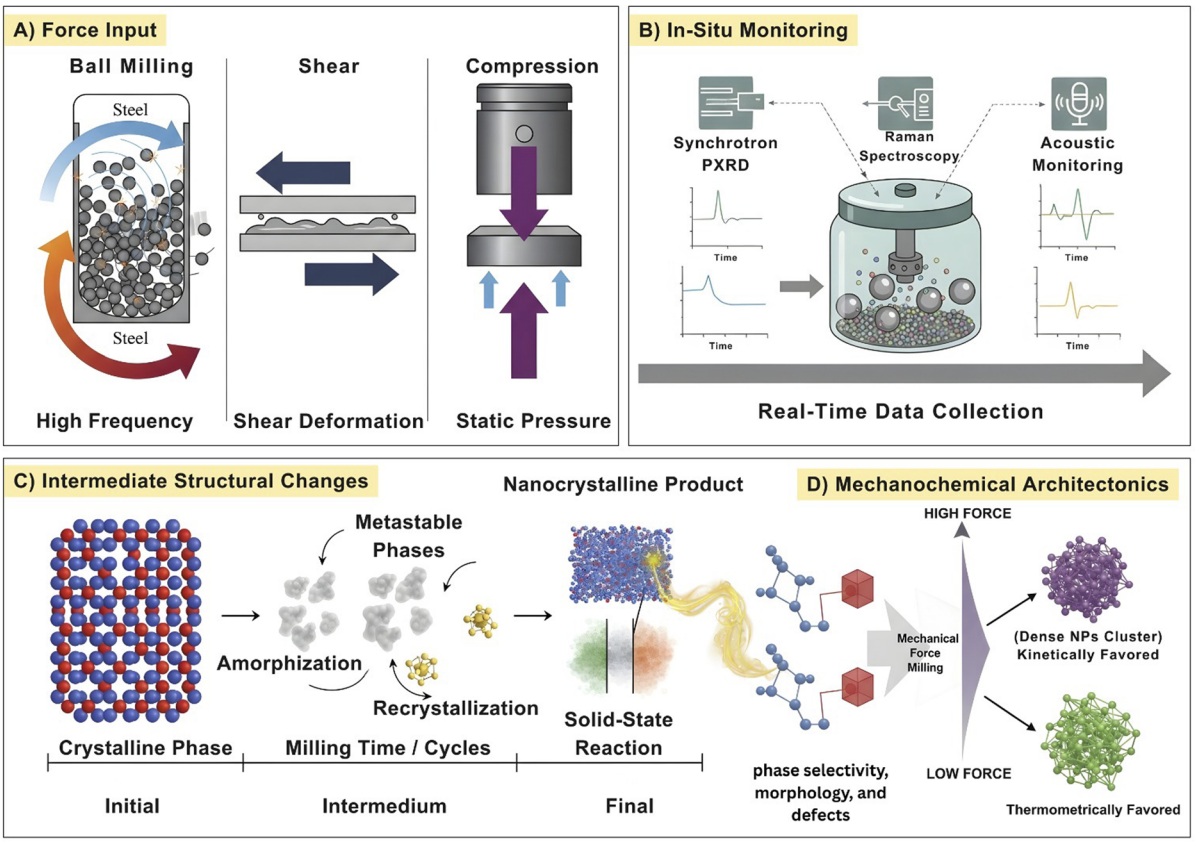

Fig. 2 (A) Mechanical force inputs in mechanochemistry, including ball milling, shear, and compression. (B) *In situ*/operando monitoring by synchrotron PXRD, Raman spectroscopy, and acoustic sensing for real-time tracking of phase evolution. (C) Force-driven structural transformations from crystalline precursors through amorphous and metastable intermediates to nanocrystalline products as a function of milling time or cycles. (D) Mechanochemical architectonics showing how force magnitude controls phase selectivity, morphology, defect formation, and final structural outcomes, distinguishing kinetically favored high-force and thermodynamically favored low-force pathways.

reproducibility across laboratories suffers, reducing mechanistic comparisons to qualitative speculation at best. For example, Belenguer *et al.*[55] emphasized that variations in jar size, shape, ball size, and materials can dramatically influence reaction outcomes even when nominal conditions remain constant highlighting the sensitive dependency of mechanochemical reactions on experimental setup specifics. Adding to this complexity, Jafter *et al.*[56] developed a kinematic modeling framework that demonstrates how even minor changes in planetary mill geometry (such as jar radius or sun wheel dimensions) can cause a 2–3× variation in impact energy, despite identical milling speed and ball load (Fig. 3A(a)). This variability stems from the way geometric parameters influence effective impact velocity, which directly affects energy transfer. Moreover, force distribution within the milling jar is inherently heterogeneous. Fig. 3A(b) illustrates how only a subset of particles experience sufficient impact energy to overcome activation barriers, creating localized (hot spots) while adjacent regions remain under-energized. This spatial disparity aligns with granular media models predicting wide force fluctuations due to varied contact angles and bead pack dynamics. Additionally, Fig. 3A(c) highlights how ball material density alters the filling factor even at constant mass affecting the total volume occupied and thus the energy delivery profile. These insights are particularly relevant for inorganic mechanochemical reactions, such as the synthesis of metal oxides (*e.g.*, TiO_2, ZnO) and intermetallics (*e.g.*, $MoSi_2$–TiC), where defect formation, phase transitions, and interface engineering are highly sensitive to localized energy input.

Moreover, force distribution within the milling environment is far from homogeneous. Particle trajectories and impact geometries create regions of intense energy concentration (hot spots) and adjacent under-energized areas (cold zones), all within the same jar. This spatial heterogeneity complicates mechanistic interpretation, as only a subset of the material may undergo defect-rich transformations while the remainder remains largely unaltered. This behavior aligns with earlier theoretical models of granular media that predict wide force fluctuations due to varied contact angles and force networks even in static bead packs.[57] De Armas *et al.*[58] quantifies how directional compressive forces mimicking ball-milling impacts affect activation energy across molecular orientations. Mechanical activation energy varied by up to 1.2 kcal mol^{-1} depending on impact direction under 2 GPa pressure, confirming the presence of "hot spots" where reactivity is enhanced. Conversely, the reverse reaction showed negligible mechanical response, illustrating "cold zones" with minimal activation. This anisotropic behavior validates granular media models predicting force heterogeneity due to variable contact angles and impact geometries (Fig. 3B).

A further limitation arises from the interplay between mechanical and thermal effects. At high frequencies, energy dissipation as heat can blur the distinction between mechanochemical and thermally assisted pathways, confounding mechanistic models. In polymer mechanochemistry, excessive force accelerates chain scission, undermining the very architectonic control sought in synthesis. Such examples highlight that more force does not necessarily mean better outcomes; instead, there exists an optimal force window where activation is maximized while degradation is minimized.[59] In a detailed investigation of oxide nanoparticle formation, Ochirkhuyag and co-workers reported that increasing the milling speed from 200 to 600 rpm raised the average collision energy from 0.1 to 0.5 J per impact, resulting in a nearly fourfold increase in defect density and a corresponding reduction in crystallite size from 45 nm to 12 nm (Fig. 3C). In the mechanochemical synthesis, that Raman bands at ~640 cm^{-1} (MnO_2), ~580 cm^{-1} (Mn_2O_3), and ~490 cm^{-1} (Mn_3O_4) evolved systematically with milling time, where extending milling from 1 h to 6 h shifted the spectrum toward the Mn_3O_4-dominant profile, quantitatively confirming the collision-driven reduction pathway induced by high-energy ball milling.[60] Similarly, Zhao *et al.*[61] demonstrated that applying higher milling frequency (30 Hz *vs.* 15 Hz) increased the lattice strain in Fe_2O_3 nanoparticles from 0.12% to 0.36%, which directly correlated with a 2.7× increase in catalytic activity for CO oxidation. These results show why controlled force input is central to defect engineering and catalytic optimization. Force modulation also governs interface formation. In the mechanochemical synthesis of TiO_2-based composites, Bharath and colleagues observed that varying the ball-to-powder ratio (5 : 1 to 20 : 1) accelerated reaction completion from 30 h down to 10 h, as more frequent high-energy collisions generated fresh interfaces and increased nucleation site density. In their solvent-free mechanochemical synthesis used Raman spectroscopy to track structural disorder and reduction, where the characteristic D and G bands provided direct evidence of defect generation and graphitic restoration under high-energy milling mirroring how increased collision intensity in other mechanochemical systems accelerates interface formation and reaction progression.[62] Importantly, these fresh interfaces were chemically distinct from bulk surfaces, hosting under-coordinated atoms that enabled selective photocatalytic activity under visible light.

Nevertheless, excessive force can be detrimental. Xiao *et al.*[63] reported that over-milling at 800 rpm caused amorphization in zinc oxide (ZnO) nanostructures, lowering photocatalytic efficiency by >35% compared to optimally milled samples. This underscores the need to define an optimal force window, where sufficient defect generation enhances reactivity but excessive impacts lead to structural collapse and loss of crystallinity (Fig. 3D). *Operando* and *in situ* studies now provide direct experimental validation of force-driven mechanisms. *In situ* synchrotron PXRD during MOF-74 ball milling reveals rapid formation of short-lived intermediates with distinct coordination motifs, where liquid-assisted grinding accelerates structural reorganization under controlled collision energies. *Operando* acoustic spectroscopy monitors mechanochemical reactions in real-time, tracking acoustic emission changes that correlate with reaction progress and energy input during ball milling.[64] The lack of standardized force quantification in mechanochemistry remains a persistent challenge, with most studies relying on indirect parameters such as rpm, ball size, or filling ratio. Li *et al.*[65] addressed this limitation by introducing the concept of specific energy dose (J g^{-1}), correlating

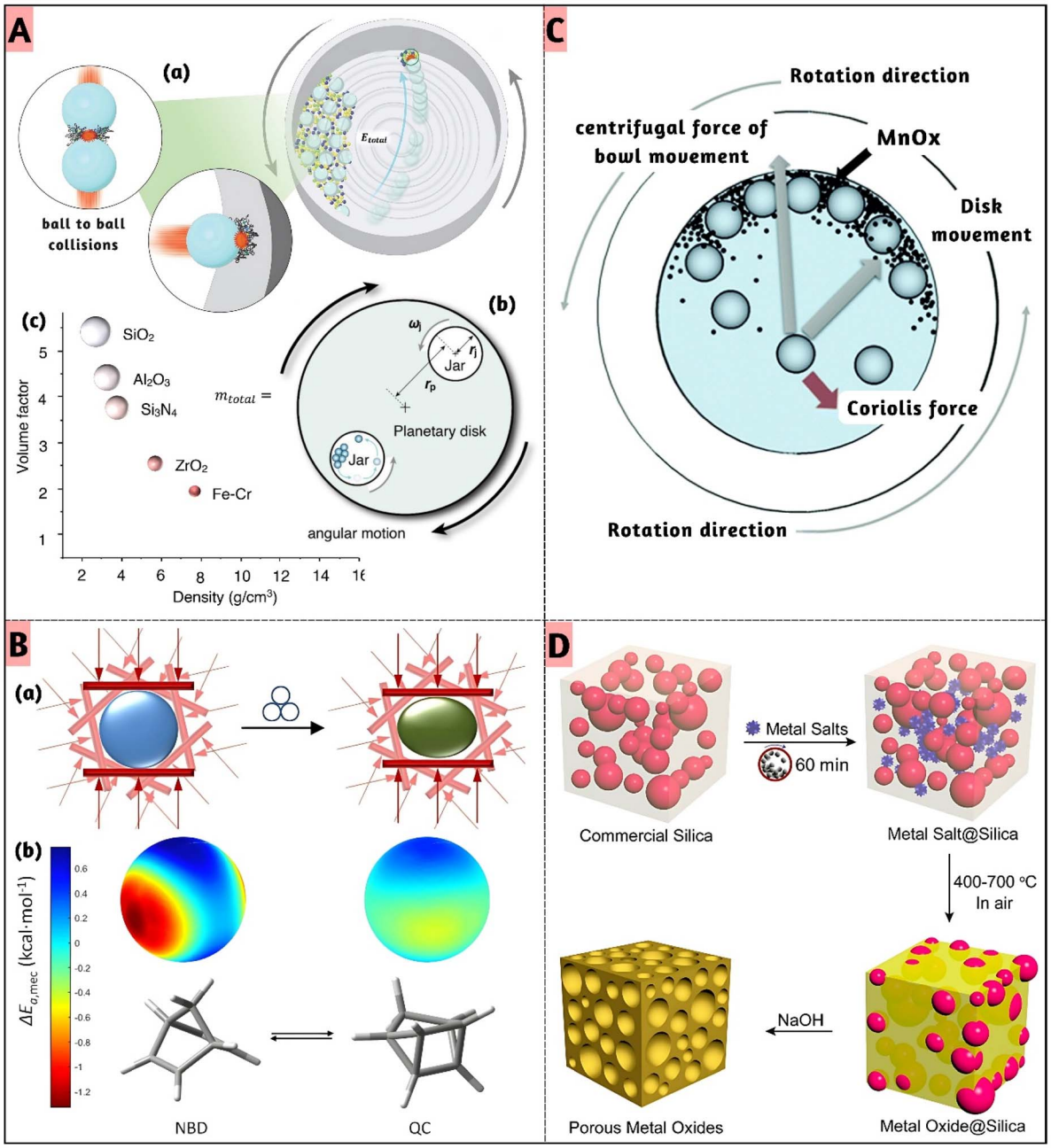

Fig. 3 (A) (a) Ball collisions during circular motion deliver mechanical energy directly to the reactant molecules. (b) The mill's illustration and the pertinent factors that affect the effective impact velocity and (c) balls have particular properties that have a direct impact on the energetics. If all ball types had the same mass, the size of the balls in the illustrations would match the relative size. Reduced with permission.[56] Copyright 2024, Wily. (B) (a) Considering all directions, random collisions drive mechanochemical reactivity to form the product. (b) (Left) Activation energy drops by ~1.2 kcal mol^{-1} under 2 GPa, indicating a "hot" mechanochemical species. (Right) Minimal response reflects a "cold" species; isomer orientations differ for clarity. Reduced with permission.[58] Copyright 2025, American chemical society. (C) Milling-map of the samples, displaying the grounding process with different ball-impact and cumulative energy which is dependent on the rotational speed. Reduced with permission.[60] Copyright 2020, Royal Society of chemistry. (D) Mechanochemical nano casting method for porous metal oxide. Adapted with permission.[63] Copyright 2018, American chemical society.

mechanical input with reaction yield across different milling platforms. In their synthesis of defective molybdenum trioxide (MoO_3), TiO_2, and ZnO, they demonstrated that a specific energy dose of approximately 1200 J g^{-1} was sufficient to induce significant oxygen vacancy formation and hydrogen doping in MoO_3, yielding localized surface plasmon resonance properties. In the archetypal mechanochemical synthesis of the metal–organic framework ZIF-8 from ZnO and 2-methylimidazole, *in situ* synchrotron PXRD measurements revealed that the distinctive Bragg reflection intensity of the (011) plane a proxy

for product crystallinity evolves markedly with milling time, showing initial formation of ZIF-8 within minutes followed by significant amorphization over *ca.* 30–40 min of continued milling (with complete amorphization observed at ~30 min under certain liquid additive conditions) and retention of crystalline features up to ~55 min with higher liquid content, demonstrating force-dependent structural kinetics directly tied to milling parameters such as liquid volume and additive concentration.[66] This time-resolved intensity profiles provide quantitative evidence that prolonged mechanical impact does not simply accelerate reactions but actively alters phase stability and pathway, consistent with mechanochemical architectonic control. Beyond diffraction, *in situ* coupled PXRD–Raman spectroscopic studies have been used to track mechanochemical reactions in real time, providing correlated structural and vibrational data that reveal the formation and consumption of intermediate phases with clear kinetic signatures as a function of mechanical input.[67]

3. Methodological platforms for mechanochemical inorganics

3.1. Ball milling and grinding architectures

Among the various mechanochemical platforms including manual grinding, liquid-assisted grinding, extrusion-based processing, high-pressure compaction, and shear-induced activation ball milling has emerged as the most widely adopted and systematically investigated architecture for inorganic synthesis, as its comminution, impact, and mixing dynamics efficiently overcome activation barriers in solid-state reactions and enable reactivity inaccessible to conventional solution-based methods.[68] Evolving from manual grinding to advanced planetary, vibratory, and Simoloyer mills, as well as scalable extrusion systems, these architectures provide enclosed, controllable environments that ensure reproducible, efficient, and adaptable synthesis across organic and inorganic frameworks.[69–71] Characteristic advantages include short reaction times, high yields, precise stoichiometric control, and the ability to proceed without bulk solvent irrespective of reactant solubility.[23,72,73] Automated mills such as shaker, planetary, and attritor devices allow programmable control of frequency and impact, while the selection of jar and media materials critically shapes frictional dynamics and mechanochemical reactivity.[32,74] Notably, LAG, defined by the η-parameter, expands the reaction scope by enhancing reactivity and selectivity.[75] This versatility is evident in the successful *in situ* preparation of hydrides such as $LiBH_4$,[76] lithium-mediated ammonia-free Birch reductions,[77] and scandium complexes unobtainable in solution.[78] Beyond molecular transformations, mechanochemical milling has proven effective in driving gas–solid reactions under ambient conditions, Lou *et al.*[79] achieved urea synthesis at a yield rate of 41.61 mg L^{-1} h^{-1} using ZrO_2 jars and balls, as schematically depicted in Fig. 4A, with earlier studies reporting ammonia generation up to 82.5 vol% and nitrogen fixation of 2.432 mg L^{-1} h^{-1}, underscoring the sustainable potential of ball–powder collisions for nitrogen conversion.

At the architectural scale, Dhokale *et al.*[80] demonstrated the critical role of milling parameters, where 7 mm balls resulted in 30% yield, while optimizing with 34 smaller 4 mm balls improved efficiency to 44% within only 99 minutes. Similarly, Marín *et al.*[81] highlighted the impact of planetary ball milling forces on catalytic activity, showing that an optimum velocity of 250 rpm maximized metal–support interactions compared to both lower- and higher-energy regimes, while the reaction atmosphere further modulated activity. Their comparative mechanistic insights are illustrated in Fig. 4B, contrasting incipient wetness impregnation with atmosphere-controlled ball milling in the preparation of Pd/CeO_2 catalysts. In another example, Zhang *et al.*[68] processed MoAlB through intensive milling at 1000 rpm for 12 h, generating amorphous phases and thinner nanosheets, followed by NaOH etching to obtain well-dispersed MBene (MB) sheets. The mechanistic sequence of lattice disruption and selective Al removal is shown in Fig. 4C, underscoring how milling can tailor nanoscale inorganic architectures.

In the context of energy storage, Shen *et al.*[82] synthesized $Na_3(VOPO_4)_2F$ nanoparticles *via* high-energy ball milling, achieving ~5 nm crystallites, *in situ* carbon-active composites, and ultralong cycling stability (98% over 10 000 cycles). This industrially scalable process (2 kg batches, 26 650 cells) is visualized in Fig. 4D, highlighting the multiscale transformation pathways accessed during solid-state milling. To establish that mechanochemical routes extend well beyond this single system, several additional force-driven syntheses have demonstrated similarly robust performance enhancements across diverse electrode chemistries.[83] For example, solvent-free mechanochemical activation has proven highly effective for Na-ion Prussian blue analogues, where reducing reaction activation energy and promoting solid-ion diffusion trigger low-temperature solid-state transformations. He *et al.*[84] showed that a Na-rich monoclinic NaMHCF cathode prepared entirely by milling exhibits high specific capacities, superior rate capability, and fully reversible multi-phase evolution during Na^+ (de)insertion representing one of the most compelling demonstrations of mechanochemistry-enabled Na-ion storage. Recent advances in all-solid-state lithium batteries provide yet another compelling line of evidence, where mechanochemical synthesis has enabled the scalable preparation of Li_3PS_4-based sulfide electrolytes with room-temperature ionic conductivities above 10^{-4} S cm^{-1} and favorable mechanical deformability that enhances solid–solid interfacial contact. Importantly, aliovalent ZnO substitution yields glass-ceramic Li_3PS_4 with significantly improved conductivity (1.12×10^{-3} S cm^{-1}) and increased stability against both air and lithium metal, illustrating how structural distortion and defect engineering introduced by force-driven processing can be leveraged to optimize ion-transport pathways and long-term cycling reliability.[85] Complementarily, Biswas *et al.*[86] demonstrated that planetary milling of halloysite-rich kaolin shortened tubular morphologies by ~44% within 1 h and ~53% within 2 h, where dry milling produced nanofragments while wet milling preserved tubular structures but still tripled surface area. As highlighted in Fig. 4E, such modifications critically regulate phosphate adsorption and release, advancing kaolin as a sustainable slow-release fertilizer carrier.

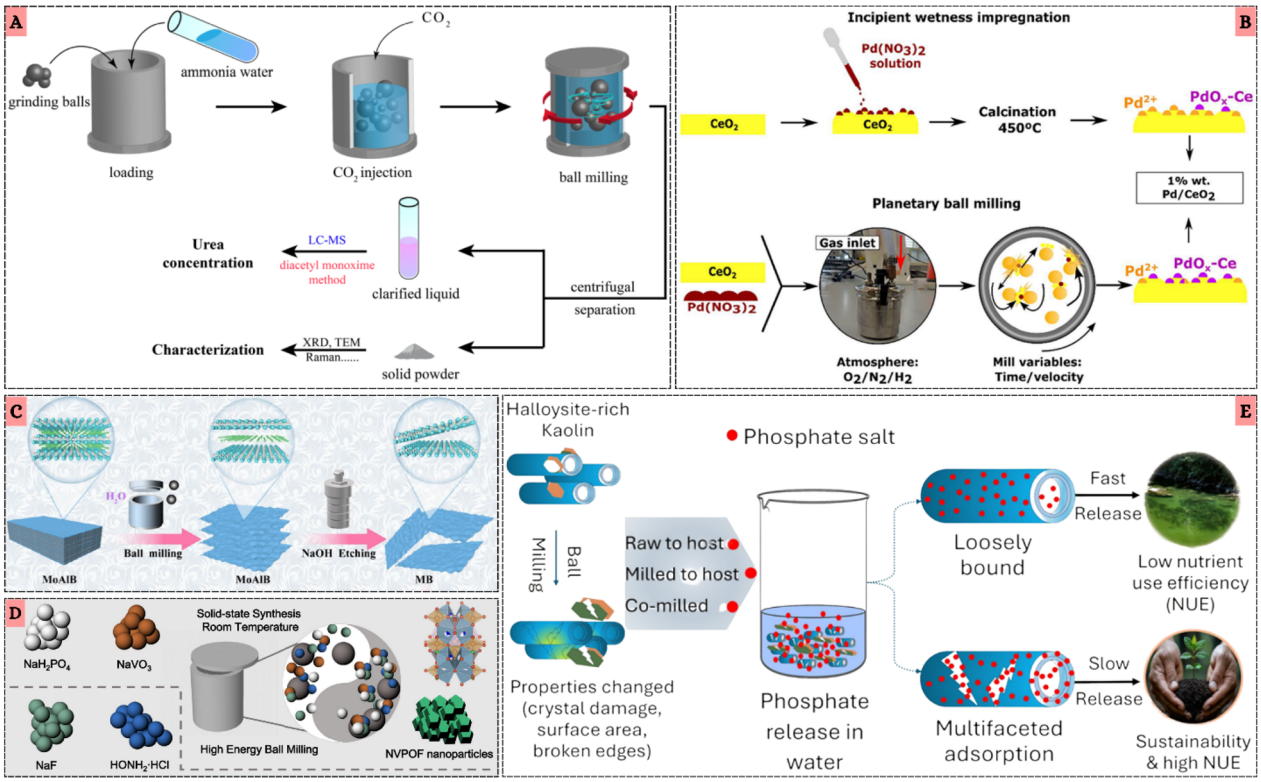

Fig. 4 (A) Schematic illustration of the urea synthesis process using ZrO_2 milling balls and a milling jar. Reproduced with permission.[72] Copyright 2025, American chemical society. (B) Illustration of the two methods used to prepare Pd/CeO_2 samples: incipient wetness impregnation and planetary ball milling under controlled atmosphere. Reproduced with permission.[74] Copyright 2025, American chemical society. (C) Synthesis flowchart of ZIF-90PN@MB. Reproduced with permission.[61] Copyright 2025, American chemical society. (D) Schematic illustration of the mechanochemical synthesis of $Na_3(VOPO_4)_2F$ nanoparticles starting from $NaVO_3$, depicting the typical synthetic process of NVPFs. Reproduced with permission.[75] Copyright 2021, Nature. (E) Schematic illustration of the mechanochemical activation of halloysite nanotube-rich kaolin clay and its application as a carrier for sustainable slow-release phosphate fertilizer. Reproduced with permission.[76] Copyright 2025, American chemical society.

Expanding further, mechanochemical strategies have enabled solvent-free C–C bond formation using Cu-complex-functionalized polyoxoniobates with high recyclability and gram-scale applicability,[87] selective mechanosynthesis of quinone derivatives with yields up to 98% through frequency and additive control,[88] and the sustainable conversion of coal-derived graphene oxide into turbostratic graphene sheets with improved purity and carbon content.[70] Ball milling has also been applied to metal–organic framework synthesis, where Plant-Collins *et al.*[89] reported optimal crystallinity and hierarchical porosity in MOF-505 within 80 minutes under reduced solvent input.

Mechanochemical synthesis of MOFs has been systematically established through neat grinding (NG), LAG, and ion- and liquid-assisted grinding (ILAG). James and Friščić[90] highlighted that direct milling of metal salts with organic linkers enables framework formation *via* force-driven solid–solid reactions, while LAG alters reaction kinetics and phase outcomes by enhancing interfacial mobility. Subsequent ILAG studies demonstrated that inorganic salt additives further regulate nucleation and polymorphism during mechanochemical MOF formation.[91] *Operando* diffraction investigations later confirmed that these force-driven routes govern MOF crystallization under solvent-minimized conditions.[92]

Environmental applications benefit as well: ball-milled MoS_2 exhibits enhanced peroxymonosulfate activation for antibiotic degradation due to defect engineering,[93] while ultrafine biochar/Fe_3O_4 composites efficiently remove pharmaceutical contaminants. In the energy domain, mechanochemical synthesis underpins cathode, anode, and electrolyte development for lithium- and sodium-ion batteries, offering improved electrochemical stability and performance.[94,95] Importantly, the sustainable production of ammonia under mild conditions *via* ball milling achieving yields of 82.5% vol. at 45 °C and 1 bar positions this platform as a compelling alternative to the Haber–Bosch process.[96] Collectively, ball milling enables the synthesis of diverse inorganic nanoparticles, including metal oxides, sulfides, carbides, perovskites, and layered compounds. Compared with liquid-assisted mechanochemistry and conventional wet-chemical routes, ball-milled nanoparticles typically exhibit nanocrystalline cores, high lattice strain, and defect-rich or partially amorphous shells, imparting unique properties such as enhanced catalytic activity, accelerated ion transport, and superior interfacial reactivity.

Taken together, ball milling and grinding architectures transcend conventional solution-based approaches by coupling tunable impact forces, scalable design, and solvent-free conditions

to activate multiscale pathways across molecular, crystalline, and hierarchical levels. By enabling sustainable nitrogen conversion, energy-relevant nanophase design, catalytic interface engineering, and environmental remediation, these mechanochemical strategies collectively exemplify how controlled impact dynamics create smart and functional interfaces, establishing ball milling as a cornerstone of mechanochemical architectonics.

3.2. Extrusion and high-pressure mechanochemistry

Extrusion-based mechanochemistry has emerged as a transformative platform for continuous and scalable solid-state synthesis, offering distinct advantages over batch milling in terms of reproducibility, process intensification, and industrial translation.[5,97–99] Its efficiency is exemplified by ZIF-8 production, which achieved a space-time yield of 144×10^3 kg per m^3 per day, far surpassing spray-cast and electrochemical routes.[5] In extrusion, ZIF-8 is prepared by feeding basic zinc carbonate and 2-methylimidazole (Zn : ligand = 2 : 3) as a dry mixture into a twin-screw extruder, where alternating conveying and kneading zones impose intense shear and compression, driving rapid solvent-free coordination between the components. Residence times of only seconds to minutes are sufficient to produce a crystalline extrudate, while controlled barrel heating (up to 200 °C) enables a melt-phase route in which the molten ligand accelerates diffusion and framework formation, yielding ZIF-8 at throughputs of 1–4 kg h^{-1}. Beyond throughput, extrusion enhances porosity and surface area compared to conventional methods,[97,98] while life-cycle assessment of ZIF-67 confirmed orders-of-magnitude lower environmental impact relative to solvothermal synthesis, underscoring its green and sustainable character.[78] Twin-screw extrusion (TSE), originally developed for polymer and food processing, has been successfully adapted to mechanochemical organic synthesis, providing a robust alternative to batch methods.[4,100] Pharmaceutical applications illustrate its power: direct amidation of esters eliminates the need for stoichiometric activating agents,[101] and Bolt *et al.*[102] achieved a 100-fold scale-up of this transformation by translating from batch ball milling to continuous extrusion.

This work further demonstrated solvent-minimized synthesis of 36 amides *via* TSE, with optimization of rheology, grinding auxiliaries, and residence time enabling long-term operation. A 7-hour run yielded ~500 g (1.3 mol) of amide at 80% yield, and the dynamics of both small-scale and extended campaigns are vividly depicted in Fig. 5, confirming extrusion's scalability and process stability.[102]

Song *et al.*[103] extended these principles through a liquid-assisted spiral gas–solid flow (LA-S-GSF) system, enabling rapid synthesis of HP-HKUST-1 at 96% yield within 11 minutes, achieving a space–time yield of 6.9×10^4 kg per m^3 per day, significantly outperforming solvothermal methods. Similarly, mechanochemical cocrystallization has produced stable pharmaceutical solids, such as ligustrazine cocrystals (TMP–MG, TMP–MG–H_2O, TMP–EG, TMP–PG), with reduced hygroscopicity and reversible solid-state interconversion, highlighting their sustainable pharmaceutical potential.[104]

Parallel developments extend into polymer and composite systems, where mechanochemical rearrangements under extrusion and high pressure preserve nanostructural porosity (>98%) and enable scalable solar water evaporation, producing 9 L per day with a 1 m^2 prototype.[105] Water-assisted gel-like extrusion of PVA achieved remarkable toughness (elongation at break 504.9%) and ultralow oxygen permeability after biaxial stretching,[106] while incorporation of NiO nanofillers into PP/PE composites enhanced tensile strength, elongation, and thermal stability.[107] Similarly, integration of caffeine-loaded UiO-66 capsules into PA6 and PLA composites *via* extrusion produced matrices with ~2.5 wt% caffeine loading and significantly improved durability relative to surface post-treatments.[108]

Complementing extrusion, high-pressure mechanochemistry exerts profound influence on atomic arrangements in solids, driving unique chemical and physical transformations.[109,110] A persistent challenge lies in controlling which mechanical strains induce specific nuclear distortions and corresponding electronic effects.[111] Recent strategies aim to tune crystal flexibility, thereby directing mechanochemical reactivity toward selective stress-responsive pathways.[112] Together, extrusion and high-pressure approaches open new frontiers for transitioning mechanochemical processes from laboratory to industry, particularly for continuous solid-state synthesis.[113,114] By coupling throughput, structural control, and environmental compatibility, these methodologies serve as critical enablers of multiscale mechanochemical pathways that underpin the design of smart and functional inorganic interfaces.

3.3. Multimodal stimuli-coupled mechanochemistry

Smart interfaces in advanced inorganic and hybrid systems are defined as adaptive material–bio interfaces that integrate stimuli responsiveness, bio-recognition, and feedback-controlled behavior, enabling dynamic modulation of interfacial structure and reactivity under external cues.[115] In this section, polymeric components are discussed only when they function as interfacial matrices or hybrid partners that directly enable the architectonic control and functional performance of inorganic nanomaterials under mechanochemical activation.

Hybrid mechanochemistry, wherein mechanical forces are synergistically combined with external stimuli such as temperature, light, ultrasound, plasma, or electric fields has emerged as a transformative strategy for accessing reaction pathways inaccessible to conventional solid-state processes.[116,117] These thermo-, sono-, photo-, and electro-mechanochemical platforms significantly broaden the chemical reactivity landscape, enabling both enhanced performance and novel functionality.[117,118] Plasma-assisted milling, for example, introduces defects into MXenes, improving their electrochemical behavior, while strain engineering under mechanochemical conditions *via* biaxial compression or out-of-plane tension has been shown to boost lithium-ion diffusion kinetics.[118,119] Hybrid protocols also facilitate *in situ* functionalization of MXenes, where stimuli-activated dopants or surface groups expand their utility in smart interfaces.[120,121]

To contextualize these differences, Table 1 provides a comparative overview of representative mechanochemical platforms in terms of energy input characteristics, scalability,

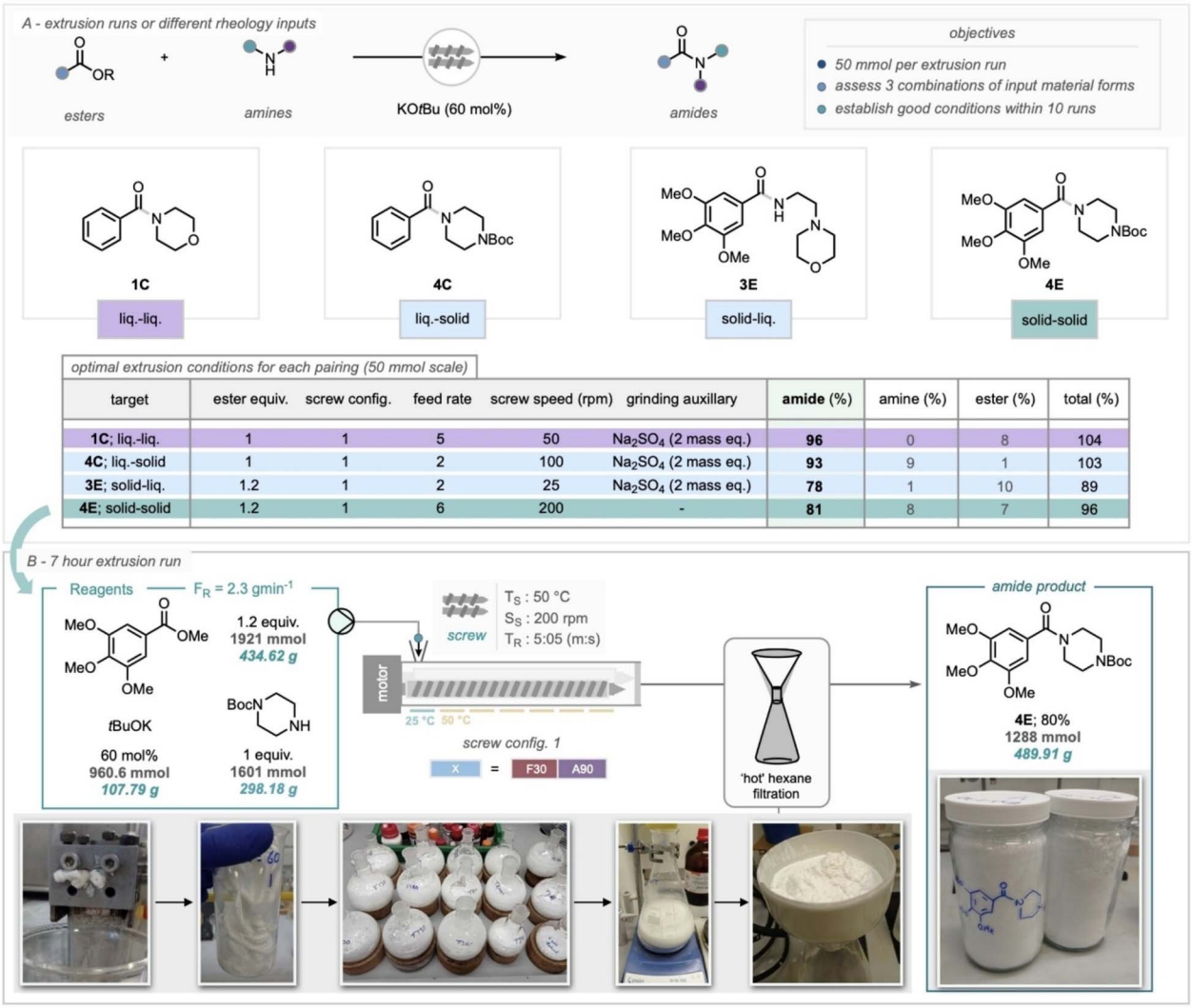

target	ester equiv.	screw config.	feed rate	screw speed (rpm)	grinding auxillary	amide (%)	amine (%)	ester (%)	total (%)
1C; liq.-liq.	1	1	5	50	Na_2SO_4 (2 mass eq.)	**96**	0	8	104
4C; liq.-solid	1	1	2	100	Na_2SO_4 (2 mass eq.)	**93**	9	1	103
3E; solid-liq.	1.2	1	2	25	Na_2SO_4 (2 mass eq.)	**78**	1	10	89
4E; solid-solid	1.2	1	6	200	-	**81**	8	7	96

Fig. 5 (A) Optimal extrusion runs of amides on a 50 mmol scale. (B) A 7-hour solvent-minimized continuous extrusion synthesis of an amide, with 30-minute batches of the extrudate collected to monitor performance over time (see SI for detailed breakdown). Reproduced with permission.[102] Copyright 2024, wiley.

and defect control. This mechanistic shift toward stimuli-activated and dynamically functionalized surfaces highlights a fundamental contrast with conventional inorganic interfaces, which respond to mechanical loading through passive pathways dominated by defect generation, microplasticity, or frictional dissipation. Traditional interfaces rely on irreversible deformation and defect-mediated reactivity characteristic of classical ball-milling or mechanically enhanced adhesion where mechanical force merely perturbs existing bonds. In contrast, smart interfaces incorporate force-responsive motifs such as mechanophores or reorganizable coordination environments that transduce mechanical, thermal, photonic, or acoustic inputs into reversible chemical rearrangements or controlled activation events. This transition from passive defect accumulation to programmable, stimuli-coupled mechanochemical behavior underpins the adaptive reactivity observed in modern thermo-, sono-, and photo-mechanochemical systems.[122,123] The fusion of ball milling with sonochemistry or photochemistry unlocks novel hybrid nanomaterials with adaptive properties.[43,124] Hwang *et al.*[125] demonstrated a mechano–chemical coupling system by integrating phospholipid copolymer vesicles within alginate hydrogels, enabling stress-induced ethylene

Table 1 Mechanochemical platforms compared through the interplay between energy delivery, scalability, and defect engineering

Platform	Energy input	Scalability	Defect control
Ball milling	High local energy, but heterogeneous	Moderate (batch-limited)	High defect density, limited precision
Extrusion	Efficient continuous energy input	High (industrial-scale)	Moderate, more uniform
Hybrid systems	Variable, stimulus-dependent	Moderate	Tunable and interface-specific

glycol tetraacetic acid (EGTA) release at only 33–55 kPa and achieving controlled degradation. On a quantum scale, Wang *et al.*[126] and Mittal *et al.*[127] used the constrained geometries simulate external force (CoGEF) method, where force application narrowed HOMO–LUMO gaps and lowered reaction barriers, highlighting the predictive power of mechanochemical simulations. Similarly, Ghose *et al.*[128] and Zhao *et al.*[129] illustrated how external solvation and ultrasound-induced piezoelectricity, respectively, modulate mechanical rupture thresholds and reactive oxygen species (ROS) generation in Zn–bis-terpyridine and Mn–ZnO hybrids. Remarkably, Qu *et al.*[130] reported that ball milling enabled MXene/PAbz hybridization *via* electrostatic and hydrogen bonding interactions, drastically reducing peak heat release rate (−69.57%) and total heat release (−54.38%), showcasing the fire-retardant promise of hybrid mechanochemistry.

Inorganic–organic hybrids can also be rapidly synthesized through silane-functionalized ball milling routes with over 90% efficiency, as reported by Amrute *et al.*[8] The solid-state synthesis of D4SB crystals *via* thermally responsive grinding,[131] and reversible emission switching, further underscores force–stimuli cooperation in tuning optoelectronic features. Structurally responsive systems such as MOFs display dynamic mechanochemical behaviors including bond rearrangement,[132] phase transitions,[133] and amorphization[134] that depend on framework topology,[135] defect density, and pore distribution.[136] Real-time tools like high-pressure crystallography and nanoindentation elucidate these force–structure couplings,[137,138] while milling experiments reveal rapid coordination bond cleavage and energy storage modulation.[139] Overall, hybrid mechanochemical systems not only offer a versatile toolbox for manipulating structure–function relationships at multiple scales but also underpin the rational design of smart and responsive interfaces for advanced inorganic materials.

4. Mechanistic insights

4.1. Multiscale reaction pathways

Mechanochemical transformations operate through inherently multiscale pathways in which atomic, interfacial, and bulk processes converge to create smart and functional interfaces. At the atomic level, mechanical input perturbs orbital overlaps, destabilizes crystal lattices, and initiates bond cleavage, generating radicals and defects that substantially lower activation barriers and activate non-thermal routes.[16,140] Ball milling exemplifies these dynamics, where localized high-energy collisions induce solid-state reactions by breaking covalent and redox bonds, decomposing surface contaminants into small molecules, and triggering vibrational excitation at transient hot spots.[141–145] Such events coalesce into a three-step progression comprising atomic-scale mixing, bond-level reorganization, and the nucleation of nanocrystalline or microcrystalline products.[4] Repeated deformation and fracture further intensify defect accumulation at grain boundaries, enabling radical generation and product nucleation under ambient conditions.[2,39] Yang *et al.*[146] extended this concept by showing that press-and-rotate mechanical inputs can reconfigure self-assembled inorganic nanorod superlattices into chiral architectures (Fig. 6A), illustrating how macroscale grinding induces nanoscale symmetry breaking with emergent optical properties.

Progressive energy input drives crystalline–amorphous transitions, where bulk structural transformations arise from bond disruption, densification, and framework collapse.[2,147–149] Localized shell formation provides both opportunities and challenges: for instance, neat milling generates nanometer-thick amorphous shells on ZnO surfaces, enhancing interfacial reactivity but also limiting further conversion by encapsulating unreacted cores.[150,151] Liquid-assisted grinding modulates this balance, as demonstrated for ZnO systems where hydrated intermediates gradually reorganize into crystalline frameworks with decreasing water content.[152] Under high pressure, Zn-imidazolate frameworks undergo selective bond cleavage and structural reorganization, collapsing pore networks while preserving short-range order.[149,153] Such cases underscore that mechanochemical reactivity does not simply replicate thermal pathways; rather, it introduces novel transformation routes linking defect accumulation, metastable polymorph formation, and bulk structural evolution.[2,154]

Mechanochemistry also provides unique avenues for coupling metal oxides and organic linkers into hybrid nanostructures. For example, solid-state reactions between ZnO and Hmim yield crystalline ZIF-8 shells encapsulating Pd nanoparticles,[155] while iron oxide precursors undergo stepwise transformations from maghemite to MOF-integrated composites *via* neat and liquid-assisted grinding.[19] Similar pathways enable metal–organic recoordination and even reconstruction of decomposed frameworks: Lee *et al.*[156] showed that ball-milling restores crystallinity and porosity in degraded MOFs such as MOF-5, MOF-177, UiO-67, and ZIF-65 through cycles of defect generation and interfacial recoordination (Fig. 6B). These insights highlight the role of mechanical force in bridging atomic-scale bond cleavage with bulk-scale structural recovery.

Beyond oxides and MOFs, mechanochemical methods have unlocked reaction channels unattainable in solution. The generation of Grignard reagents from fluoronaphthalenes,[157] the activation of benzene through Mg(I) dimers,[69] and the stabilization of unusual η^3-allyl–Mg coordination modes[158] exemplify bond activation pathways arising directly from mechanical inputs. Likewise, lignin depolymerization under milling produces stable phenoxy radicals that reduce metal ions and initiate unconventional bond transformations.[16] At higher scales, metal alloys and nitrides undergo progressive grain refinement, defect accumulation, and hot-spot-assisted diffusion, as shown for Fe–Cr–Si alloys and TiN formation.[6,159] These cases emphasize that interfacial charge gradients, radical fluxes, and nanoscale strain collectively govern reactivity in ways decoupled from conventional thermal dynamics.[39,97,142]

Hybrid mechanochemistry further expands this framework by integrating force with external stimuli, enabling hierarchical transformations across multiple scales. Cheng *et al.*[160] reported a nanocasting route in which lattice-level Mn incorporation into CeO_2 generated mesostructured $CeMnO_x$ catalysts, achieving nearly complete NO_x conversion at 150 °C and highlighting the solvent-free scalability of this process (Fig. 6C). Zhang *et al.*[161]

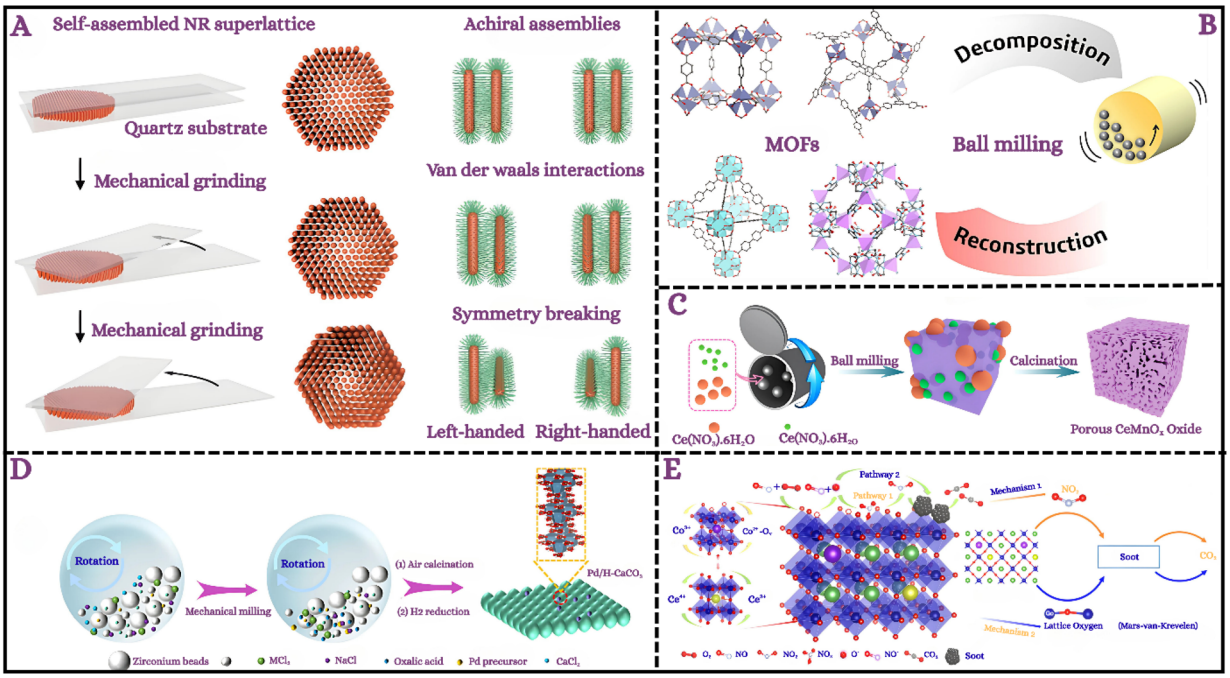

Fig. 6 (A) Schematic illustration of chirality generation in self-assembled NR superlattices *via* a press-and-rotate mechanical force. Reproduced with permission.[146] Copyright 2022, Nature. (B) Schematic of MOF transformation *via* ball milling, showing framework decomposition followed by structural reconstruction. Reproduced with permission.[156] Copyright 2021, American chemical society. (C) Schematic illustration of mechanochemical nanocasting synthesis of porous $CeMnO_x$ catalysts. Reproduced with permission.[160] Copyright 2019, American chemical society. (D) Process of the preparation of MCO_3.[161] Copyright 2023, American chemical society. (E) Schematic of La (Ce,K)CoO_3 lattice and redox cycles, highlighting soot oxidation *via* Langmuir–Hinshelwood and Mars–van Krevelen mechanisms. Reproduced with permission.[162] Copyright 2022, American chemical society.

demonstrated that salt-assisted milling engineers hierarchical porosity in carbonates, where lattice perturbations, NaCl templating, and pore evolution converge to confine Pd nanoparticles within $CaCO_3$ matrices (Fig. 6D). Yu *et al.*[162] advanced the concept by designing alkali/cerium co-modified La–Co perovskites that exploit coupled atomic redox cycles, interfacial oxygen vacancy dynamics, and bulk lattice oxygen participation. *In situ* DRIFTS and DFT revealed synergistic Langmuir–Hinshelwood and Mars–van Krevelen mechanisms, with (Fig. 6E) illustrating how bifunctional effects in soot combustion catalysis arise from coordinated atomic, interfacial, and bulk processes.

These multiscale pathways reveal that mechanochemistry does not merely replicate thermal dynamics but opens unconventional reaction channels. However, the lack of a comprehensive quantitative framework limits predictive control over outcomes. The critical challenge remains to bridge atomic and interfacial events with bulk transformations through integrated modeling for rational design of smart interfaces.

4.2. Computational modeling and AI integration

Computational modeling has become indispensable for unraveling mechanochemical pathways, yet the diversity and complexity of applied forces render atomistic simulations inherently challenging. Classical frameworks such as Bell's model have long provided first approximations to reaction energy modifications,[163] while more advanced strategies such as the CoGEF method quantify force-dependent energy variations by relaxing perturbed systems between pulling points.[164] These efforts underscore that truncated model risk overlooking stereochemical contributions, since computational predictions of activation lengths for *E*- and *Z*-alkene isomers (1.65 Å and 1.24 Å) closely match experimental values (1.67 ± 0.05 and 1.20 ± 0.05 Å), affirming the cusp model's utility in describing reaction potential energy surfaces despite qualitative assumptions.[164] Recent developments, such as steepest-descent pathways (SDPs), further refine predictive capabilities by offering efficient yet experimentally validated approximations of mechanochemical reaction rates.[165] Bunno *et al.*[166] elegantly demonstrated this principle by employing DFT within the push–pull protonated atomic distance (PAD) framework to predict proton conductivity in acid–base hybrids. As shown in Fig. 7A, incorporation of TiO_2 shortened PAD values, reorganized hydroxyl groups, and promoted proton hopping cascades, thereby guiding the rational design of proton-conducting inorganic–organic hybrids. Parallel work by Wu and Wang[167] extended this paradigm to hybrid organic–inorganic perovskites (HOIPs), where a progressive machine learning framework integrated enriched input databases with DFT validation. As presented in Fig. 7B, their models spanned diverse A-site cations, B-site metals, and X-site anions, with band-gap distributions confirming robust predictive accuracy across metals, semiconductors, and insulators.

Complementary to these approaches, quantum chemistry calculations have revealed molecular deformation during

activation, with the extreme-pressure polarizable continuum model tracking cavity volume changes under hydrostatic stress,[168] while density functional theory (DFT) demonstrated how mechanical stress deforms C–C bonds, enabling thermally forbidden electrocyclic reactions.[169] At the mesoscale, computational studies show that forces applied orthogonally to the reaction coordinate can significantly alter transition-state curvature,[170] though no current model fully quantifies the mechanical work exerted during ball milling.

Nonetheless, recent work by Pladevall *et al.*[171] has shown that standard DFT combined with continuum solvation and microkinetic modeling can quantitatively describe ball-milling reactions. By treating mechanochemical conditions as solution-like reactions with modified effective concentrations and dielectric

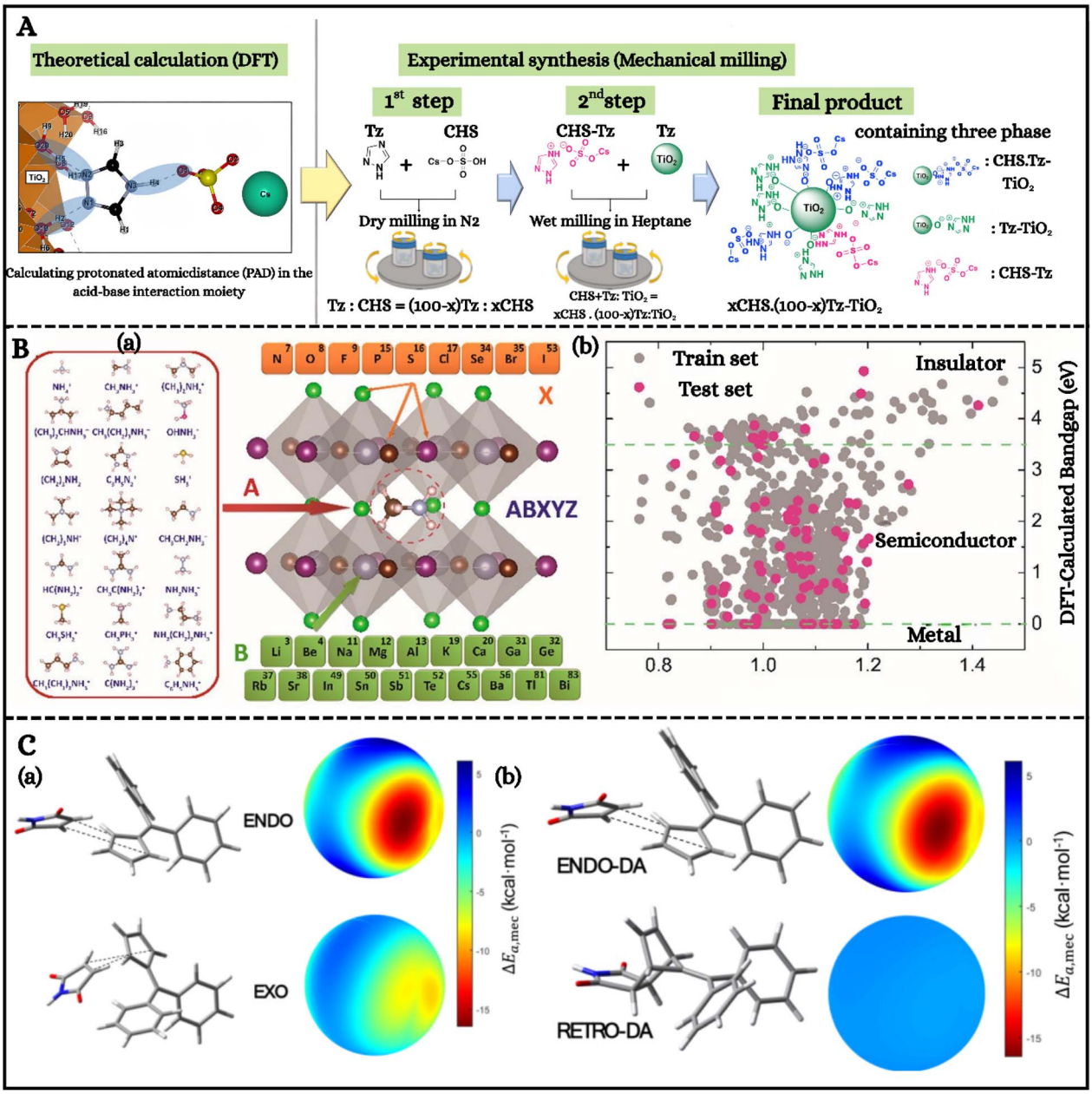

Fig. 7 (A) Schematic representation of the procedure for developing proton-conducting inorganic–organic hybrids, guided by computational modeling. Reproduced with permission.[166] Copyright 2023, American chemical society. (B) (a) Dataset construction for HOIP prediction, comprising 21 monovalent organic molecular cations (A-site), 19 metallic cations, and 9 representative anions across the periodic table. (b) Visualization of training (gray dots) and test (red dots) data based on tolerance factor and DFT-calculated band gap (PBE), illustrating the coverage of metals, semiconductors, and insulators within the dataset. Reproduced with permission.[167] Copyright 2020, American chemical society. (C) (a) (Top) *Endo* adduct and its spherical representation of $\Delta E_{a,mec}$ as a function of wall-type force directions. Some impact directions reduce the activation energy by up to −16.5 kcal mol^{-1}, with an average $\langle \Delta E_{a,mec} \rangle$ of −3.88 kcal mol^{-1}. (Bottom) *Exo* case, showing a maximum reduction of −8.9 kcal mol^{-1} and an average $\langle \Delta E_{a,mec} \rangle$ of −2.89 kcal mol^{-1}. (C) (b) Comparison of activation energy variations for the *endo* Diels–Alder reaction (top) and the retro-DA reaction from the *endo* product (bottom). The mechanical effect on the retro-DA reaction is nearly negligible, as reflected in the $\Delta E_{a,mec}$ scale. (C and D) Reproduced with permission.[58] Copyright 2025, American chemical society.

constants, they reproduced experimentally observed reaction times for Diels–Alder cycloadditions and *N*-sulfonylguanidine formation under ball milling, and concluded that, at least for these benchmark systems, the mechanisms under milling and in solution are essentially identical and amenable to DFT-based analysis. Moreover, dispersion-corrected DFT has been directly applied to ball-milling conditions themselves, as demonstrated by Rojas-Chávez *et al.*,[172] who computed ligand–surface interactions, surface-energy shifts, and facet stabilization in PbTe nanoparticles during high-energy milling.

Molecular dynamics further illuminate surface and interfacial pathways, exemplified by alkyl thiolate interfaces on coinage metals, where shear generates distinct metal-containing species and governs stress-driven surface-to-bulk transport.[173] Fusaro *et al.*[174] advanced this direction by developing a DFT-based framework incorporating electrostatics and solvent effects, successfully predicting ~20 kcal mol^{-1} binding energies for biomolecule–gold interactions, consistent with experiments. Importantly, such mechanistic insights extend directly to nanoscale biointerfaces, as demonstrated by Triatmaja *et al.*,[175] whose DFT-optimized docking models clarified the antibacterial mechanism of GO/ZnO/eugenol composites, revealing strong binding (−11.65 kcal mol^{-1}) to DNA gyrase and effective ATP blockade.

To capture milling dynamics more holistically, discrete element method (DEM) and structural phase-field-crystal (XPFC) models have been employed. By incorporating ballistic terms, XPFC simulations reproduced nanoparticle nucleation and growth trends under room-temperature milling, with ligand chain length modulating the free energy landscape and predicting reduced particle sizes for longer ligands.[176] Further refinement of reaction selectivity under mechanical stress has been achieved through mechanochemical algorithms. For example, diphenylfulvene/maleimide systems under isotropic wall-type forces showed preferential *endo*-pathway stabilization, with $\langle \Delta E_{a,mec} \rangle$ reductions of −3.88 kcal mol^{-1} compared to −2.89 kcal mol^{-1} for the *exo* case, offering a microscopic rationale for experimentally observed *endo* selectivity in mechanochemical Diels–Alder reactions (Fig. 7C(a)).[58] Strikingly, retro-Diels–Alder processes remained unaltered, confirming that force biases are pathway-specific (Fig. 7C(b)). Collectively, these computational strategies from CoGEF and SDPs to DEM and XPFC demonstrate how stress can reshape potential energy landscapes, drive bond rupture (C–C, Si–O, S–Au), and rationalize transformations inaccessible by purely thermal means.

The integration of artificial intelligence (AI) has further accelerated progress, enabling optimization of mechanochemical conditions and predictive modeling with unprecedented precision. Machine learning potentials now reconcile the accuracy of quantum methods with the efficiency of classical simulations, resolving long-standing trade-offs.[177] Algorithms such as XGBoost, coupled with dimensionality reduction, achieve up to 80% predictive accuracy in mechanochemical cocrystallization, outperforming conventional approaches and highlighting electrostatics and structural compatibility as AI-derived guidelines for rational solvent-free design.[178] Artificial neural networks (ANNs) extend this capability, with models trained on process parameters and formulations achieving $R^2 > 0.99$ for predicting pharmaceutical cocrystallization during ball milling. Such predictive robustness motivates hybrid models that fuse mechanistic frameworks with AI, enhancing accuracy in simulating complex multi-component systems.[179] Beyond organics, computational chemistry paired with AI has successfully predicted defect energetics, binding affinities, and electronic behaviors in inorganic nanomaterials ranging from metal oxides to sulfur-based systems,[159,180] underscoring cross-material generality. Together, computational modeling and AI not only decode multiscale mechanistic pathways but also enable rational control of smart functional interfaces, establishing a predictive foundation for the design of next-generation inorganic nanomaterials.

5. Unlocking smart and functional interfaces

5.1. Catalysis and energy interfaces

Mechanochemical architectonics offers a revolutionary approach to the design of catalytic and energy interfaces, wherein structural evolution-characterized by flaws, porosity, and dopant distribution-occurs directly under mechanical force. Mechanochemical processing, unlike traditional synthesis, works in solvent-free or low-solvent environments. This lets you quickly get to nonequilibrium states with high defect concentrations, nanocrystallinity, and close contact between components-things that are frequently hard to get using traditional methods.[181] This force-driven environment fosters oxygen migration, accelerates redox cycling, and enhances selective adsorption, leading to the development of "active microreactors" on the material surface that improve catalytic responsiveness. Crucially, mechanochemical routes allow direct tuning of active site structures-vacancy-rich surfaces, hierarchical pores, and atomically dispersed dopants. This means that solvents, templates, or high-temperature procedures are not needed, which is in line with the ideas of green chemistry and scalable synthesis.[23,182]

Siniard *et al.*[183] indicated that incorporating CuCoFeNiMnO_x into a CeO_2 lattice using ultrasound-driven lattice engineering generates numerous oxygen vacancies, well-dispersed cations, and enhanced Ce^{3+}/Cu^{+} redox centers. These characteristics facilitated ultralow-temperature CO oxidation (T_{50} = 100 °C, T_{100} = 150 °C), exceeding traditional dense HEOs. Fig. 8A demonstrates that the catalytic cycle involves lattice oxygen migration, vacancy formation, and fast oxygen replenishment, exemplifying a Mars–van Krevelen mechanism that imparts remarkable activity and stability to the HEO–CeO_2 interface. Similarly, Zhang *et al.*[161] devised a salt-assisted mechanochemical method to synthesize porous $CaCO_3$, $SrCO_3$, and $BaCO_3$ in few minutes, attaining unprecedented surface areas (up to 172 m^2 g^{-1}). The Pd-loaded hierarchical $CaCO_3$ catalyst achieved nearly total nitrobenzene hydrogenation (≥99% yield, TON = 1.3 × 10^4 h^{-1}) and shown exceptional reusability throughout 11 cycles. Fig. 8B illustrates that NaCl templating during milling facilitates pore development, resulting in stable,

high-surface-area interfaces conducive to effective catalysis. Furthermore, Xiao *et al.*[184] developed an innovative method for extracting gold from anode slime without the use of solvents. This process involves $KMnO_4$ and NH_4Cl generating reactive chlorine species during milling, which oxidize metallic Au into soluble $AuCl_3$. This approach was highly selective and yielded numerous results without employing toxic cyanide or solvent-intensive methods. This illustrates how mechanochemistry may benefit the environment through resource reutilization. Fig. 8C illustrates that the mechanical activation of $KMnO_4$ and NH_4Cl in conjunction results in the release of chlorine, facilitating the direct conversion of gold at ambient temperature. Likewise, Zhan *et al.*[185] described a template-free mechanochemical method for synthesizing mesoporous CuO_x–CeO_2, with surface areas of up to 122 m^2 g^{-1} with interconnected pores measuring 2–5 nm. The sponge-like structure maintained atomic-scale Cu^{2+} dispersion and improved Cu^{2+}/Cu^{+}–Ce^{3+}/Ce^{4+} redox cycling, facilitating complete CO oxidation at around 98 °C, as illustrated in (Fig. 8D). Yang *et al.*[186] developed a solvent-free mechanochemical approach for synthesizing Fe_3O_4

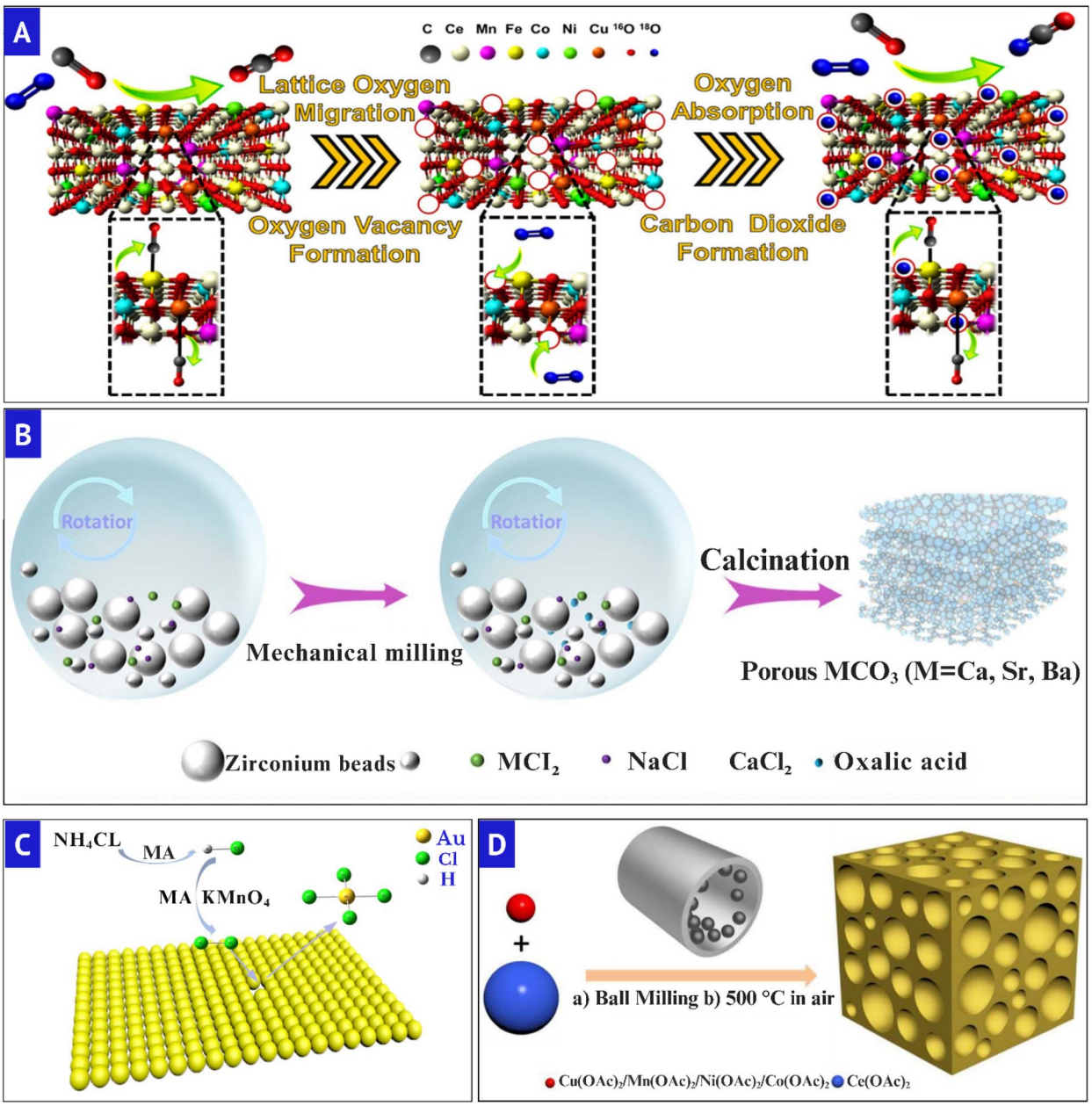

Fig. 8 (A) Illustration of the synergistic HEO-assisted Mars–van-Krevelen mechanism for 0.25-HEO–CeO_2. Reduced with permission.[183] Copyright 2024, American chemical society. (B) Process of the preparation of MCO_3 *via* salt-assisted mechanochemical milling and calcination. Reduced with permission.[161] Copyright 2023, American chemical society. (C) Mechanism of gold conversion using $KMnO_4$–NH_4Cl through the mechanochemistry approach (MA). Reduced with permission.[184] Copyright 2019, American chemical society. (D) Illustration of mechanochemical synthesis of mesoporous CuO_x–CeO_2 and transition-metal-doped ceria catalysts. Reduced with permission.[185] Copyright 2017, American Chemical Society.

nanoparticles, distinguished by many oxygen vacancies and Fe^{2+}/Fe^{3+} redox centers, which promote improved chemoselective reduction of nitroarenes. This catalyst, produced using ball milling and characterized by numerous flaws, exhibited over 99% selectivity, commendable turnover efficiency, and excellent reusability after 10 cycles. The engineered contact inhibited sintering, preserved the crystals, and facilitated electron mobility among them. All of them are crucial for energy-related catalytic applications. This study demonstrates how mechanochemistry can produce catalytic surfaces that are both physically robust and functionally superior.

5.2. Biomedical interfaces

Mechanochemical architectonics is gaining prominence as a method for constructing biomedical interfaces, where stability, biocompatibility, and multifunctionality are paramount. Conventional synthetic methods sometimes encounter issues such as limited dispersibility, cytotoxicity, or loss of functionality under physiological conditions, complicating the application of nanomaterials in clinical environments. By contrast, mechanochemistry enables direct control over surface functionalization and hybridization, producing defect-rich, coated, or host–guest-modified nanostructures without the need for harsh solvents or complex templating.[187] Beyond improving safety profiles, mechanochemical engineering also unlocks smart functionalities at the bio-nano interface, ranging from enhanced antioxidant performance to controlled release and protective exoskeletons. Hybrid coatings and supramolecular assemblies formed *via* mechanical activation can safeguard sensitive biomolecules and impart them with innovative abiotic characteristics such as magnetism, fluorescence, or UV resistance. These attributes are essential for bioimaging, biosensing, and therapeutic systems. These advancements demonstrate that mechanochemistry transcends conventional boundaries of nanoparticle coatings, extending into living cell encapsulation, drug delivery, and biomedical protective technologies.[2,188]

Here, biomedical interfaces are approached from an inorganic-centered perspective, where organic and supramolecular elements are introduced as functional enablers to tailor surface chemistry, protection, and biointeractions of nanomaterials rather than as standalone material systems. Krupiński *et al.*[189] introduced a mechanochemical strategy to produce sub-10 nm ZnO nanocrystals stabilized with urea ligands, demonstrating how surface chemistry can be tuned during synthesis to achieve stable organic–inorganic interfaces. A subsequent modification of β-cyclodextrin (β-CD) conferred

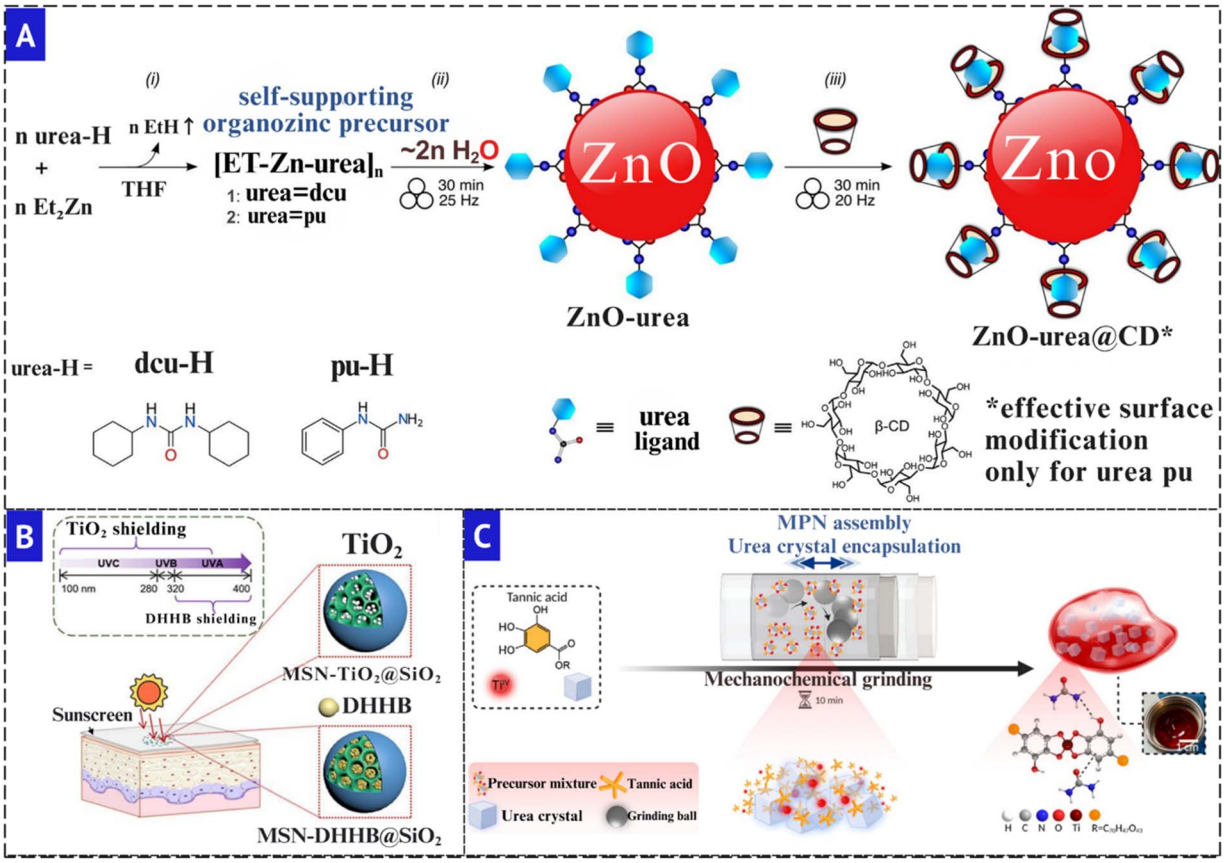

Fig. 9 (A) Mechanochemical synthesis of ZnO nanocrystals from ethylzinc–ureate precursors and postsynthetic β cyclodextrin (β-CD) modification for water solubility. Reduced with permission.[189] Copyright 2021, American chemical society. (B) Schematic structures and advantages of solid SiO_2-sealed filter-entrapped MSNs (MSN-TiO_2@SiO_2 and MSN-DHHB@SiO_2) and their UV protection mechanism. Reduced with permission.[190] Copyright 2023, American chemical society. (C) Schematic of the mechanochemical, coordination-driven assembly of MPNs for urea crystal encapsulation. Reduced with permission.[191] Copyright 2023, American chemical society.

water solubility and enhanced bioprocessability, essential conditions for the biomedical application of ZnO nanoparticles. Fig. 9A demonstrates the sequential process-from urea precursors to ZnO–urea nanocrystals and ultimately β-CD functionalization-demonstrating how mechanochemistry facilitates the synthesis of nanostructures specifically designed for biomedical interfaces, where dispersibility and compatibility are crucial. Similarly, Ma *et al.*[190] engineered solid SiO_2-sealed mesoporous silica nanoparticles to co-encapsulate TiO_2 and the organic UV filter DHHB, attaining broad-spectrum protection while inhibiting ROS release and skin penetration. The coating method demonstrated stability and safety in sunscreen applications, as illustrated in Fig. 9B. Likewise, Mazaheri *et al.*[191] illustrated a solvent-free mechanochemical method for encapsulating urea within metal–phenolic networks (MPNs), wherein tannic acid coordinated with Ti^{4+} during grinding to create stable hybrid matrices. As illustrated in (Fig. 9C), the resultant coatings demonstrated adjustable stability and regulated release, underscoring how mechanochemistry facilitates biocompatible and protective interfaces, akin to β-cyclodextrin-modified ZnO nanocrystals and silica-encapsulated UV filter systems.

To ensure consistency with the catalysis and energy sections, this section now emphasizes direct mechanism–function relationships at the bio–nano interface. In particular, mechanochemically induced surface defects, ligand coordination modes, and hybrid architectures are explicitly correlated with biological performance metrics such as biocompatibility, oxidative stress modulation, and cellular uptake behavior. A comparative overview of mechanochemical and conventional synthesis routes is provided in Table 2.

The clinical relevance depends on a clearer understanding of their *in vivo* behavior, safety profile, and regulatory positioning. Recent studies demonstrate that solvent-free architectures, including metal–phenolic networks and ligand-passivated oxide nanostructures, display enhanced serum stability, reduced aggregation, and predictable degradation pathways, resulting in improved biodistribution and biocompatibility *in vivo*.[198,199] The stability and safety attributes correspond closely with the current expectations of the U.S. Food and Drug Administration (FDA) and European Medicines Agency (EMA), especially for the reduction of organic solvent residues, impurity control, and reproducibility in nanomaterial production.[200,201] Mechanochemistry, being a solvent-free and energy-efficient process, automatically meets numerous regulatory standards, making it a compelling option for future nanomedical production pipelines.[202]

Beyond conventional nanocarriers, mechanochemistry is accelerating the emergence of drug–nanomaterial composite strategies that hold significant value for pharmaceutical and clinical translation. Mechanochemical co-crystallization has enabled the formation of drug–excipient pharmaceutical co-crystals that improve solubility, dissolution kinetics, and physicochemical stability.[203–205] Moreover, solid-state amorphization *via* high-energy milling generates amorphous drug phases that exhibit improved bioavailability and regulated release characteristics, thereby obviating the necessity for organic solvents or high temperatures.[206] Collectively, these advancements underscore the capacity of mechanochemistry to produce biocompatible, stable, and therapeutically pertinent solid-state drug–nanomaterial hybrids, hence enhancing the translational potential of the mechanochemical platforms outlined in this section.

5.3 Electronics and sensing interfaces

Mechanochemical strategies are increasingly redefining the design of electronic and sensing materials by enabling solvent-free, force-driven construction of functional interfaces with atom-level precision. These technologies provide sustainable, scalable approaches to develop heterojunctions, doped frameworks, and responsive structures that are meticulously

Table 2 Mechanochemical versus conventional synthesis routes and their impact on surface properties and biological performance

Aspect	Mechanochemical synthesis	Conventional synthesis	Biological mechanism–function correlation	References
Surface structure	Defect-rich, force-activated interfaces with tunable coordination	Thermodynamically relaxed surfaces	Controlled defects reduce cytotoxicity	189
ROS behavior	Defect passivation and solid-state ligand binding suppress ROS	Unpassivated surfaces promote ROS formation	Lower oxidative stress improves cell compatibility	192
Surface chemistry	Strong solvent-free ligand anchoring	Weak post-synthetic coatings	Enhanced dispersion and stability	193
Colloidal stability	Clean interfaces minimize aggregation	Residual solvents increase agglomeration	Reduced immune activation	97 and 194
Biocompatibility & hemocompatibility	Cleaner surfaces (no solvents), strong ligand anchoring → higher compatibility	Residual solvents, surfactants → potential cytotoxicity	Mechanochemical coatings significantly improve biocompatibility and reduce cellular stress	195–197
Drug encapsulation & release profiles	Solid-state assembly of metal–phenolic networks (MPNs) yield sustained release	Sol–gel and emulsion routes often show burst release	Mechanochemical MPNs provide controlled and stable release profiles	191

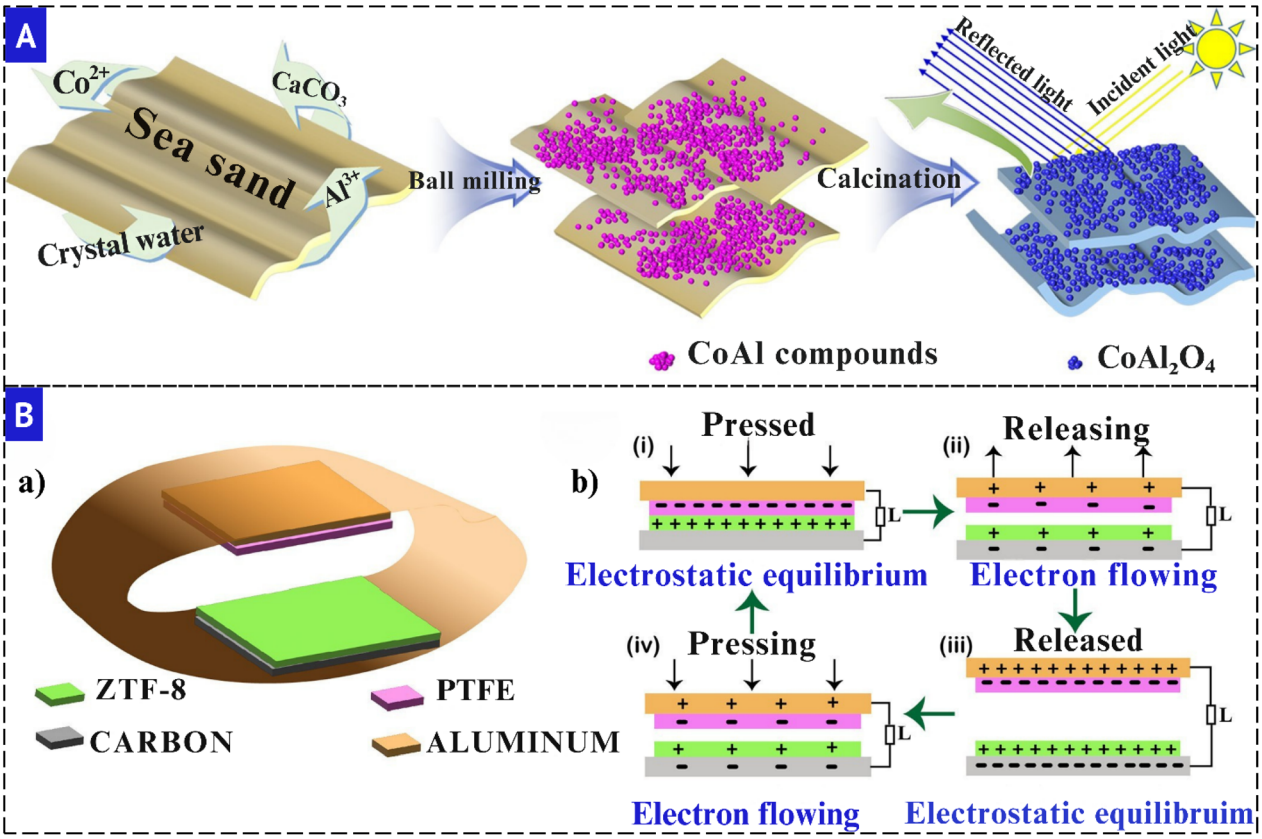

Fig. 10 (A) Schematic diagram of the preparation of $CoAl_2O_4$ composite pigments *via* a $CaCO_3$-assisted mechanochemistry method followed by calcination. Reduced with permission.[209] Copyright 2022, American chemical society. (B) (a) Schematic diagram of the proposed ZTF-TENG device architecture, in which ZTF-8 acts as the triboelectric positive material and PTFE as the negative counterpart, layered with carbon and aluminum electrodes for flexible operation. (b) Schematic of the contact–separation mechanism, illustrating charge generation and electron flow during device operation. Reduced with permission.[210] Copyright 2024, American chemical society.

optimized for enhanced charge transfer, selective analyte interaction, and signal transduction. Mechanochemically synthesized devices have demonstrated potential in the creation of self-powered gas sensors, vibrational energy harvesters, and chemiresistive and luminous detectors, which are crucial for applications spanning environmental monitoring to smart wearables. As the demand for miniaturized, flexible, and intelligent sensing modalities grows, mechanochemical interface engineering stands out as a transformative platform capable of unlocking next-generation transduction technologies.[116,207,208]

Yang *et al.*[209] devised a more environmentally friendly mechanochemical method for producing $CoAl_2O_4$ composite pigments through the ball-milling of sea sand, $CaCO_3$, and metal nitrates, succeeded by calcination. Fig. 10A illustrates that the $CoAl_2O_4$ nanoparticles were affixed to quartz surfaces, augmenting blue-light reflectance (~430 nm) *via* interface-induced scattering. This sustainable technique diminished cobalt use while attaining superior optical stability, indicating prospective applications in colorimetric sensors, NIR-reflective coatings, and functional inks. In another study by Sarfudeen *et al.*[210] engineered a mechanochemically manufactured triboelectric nanogenerator (TENG) utilizing ZTF-8 (a zeolitic tetrazolate framework) combined with carbon, resulting in a flexible, layered interface for energy harvesting and sensing. Fig. 10B illustrates that the TENG incorporates layers of PTFE, aluminum, ZTF-8, and carbon, which cyclically accumulate and discharge surface charge during mechanical contact and separation. This arrangement facilitates alternating electrostatic equilibrium and electron flow, yielding an output of 65 V and 4.2 μA, demonstrating exceptional responsiveness to human motion. Qin *et al.*[211] fabricated Se-doped MoS_2/ZnO heterostructures by a mechanochemical approach, incorporating both substitutional and interstitial selenium atoms to improve NH_3 detection at ambient temperature. The dual-site doping enhanced charge transfer, surface reactivity, and heterojunction integrity, yielding a sixfold increase in sensitivity, a detection limit of 25 ppb, and expedited reaction and recovery times. Hidalgo-Rosa *et al.*[212] employed multiconfigurational *ab initio* calculations to elucidate the luminescence quenching mechanism in nitroaromatic-responsive lanthanide MOFs, demonstrating that strong host–guest electronic coupling perturbs the antenna-to-metal energy-transfer pathway. Theoretical analysis revealed that π–π interactions and analyte-induced destabilization of the ligand triplet state suppress Tb^{3+} sensitization, resulting in efficient turn-off luminescence behavior and high sensing selectivity toward nitro compounds.

6. Challenges and future perspectives

6.1. Current limitations

Mechanochemistry, though eco-friendly and capable of reducing solvent use, still faces critical challenges that constrain its broader application in designing smart and functional interfaces. Nanostructured oxides obtained through mechanochemical routes often contain a high fraction of structurally disordered interfaces, which complicates the separation of bulk and surface contributions,[213] while diffraction techniques lose much of their resolving power in such nanoscale and disordered systems, making atomic-scale resolution particularly difficult. Mechanically induced phase transformations strongly depend on milling dynamics, rendering reproducibility and kinetic control difficult,[151] and subsequent thermal relaxation alters functional properties, thereby compromising reliable performance in practical applications. Achieving consistent and reproducible reactions is further hindered by variable parameters such as temperature, pressure, and milling intensity,[144] while localized heating at impact points often triggers unintended side reactions or precursor decomposition.[214] Reports on nanoparticle synthesis must also be interpreted cautiously, as XRD frequently underestimates particle sizes compared to catalytically relevant surface features.

The inherent simplicity of mechanochemistry masks persistent issues: processes often proceed on a trial-and-error basis due to the absence of a comprehensive predictive framework,[9] and current models including hot spot and magma–plasma theories remain qualitative, failing to integrate mechanical energy into thermodynamic formalisms. Existing nanoparticle growth models from dilute solutions cannot be directly applied to solid-state systems,[176] and no current theory adequately describes the spatiotemporal evolution of nucleation or nanocrystalline precipitates. Consequently, rational design remains limited, and reaction selectivity is frequently undermined by unintended side reactions.[215] These challenges are compounded by the restricted scope of mechanochemical transformations, as reactions requiring precise temperatures, pressures, or solvent participation often fall beyond the reach of mechanical activation.[144,215]

Practical synthesis also faces substantial barriers. Multistep and solvent-intensive methods raise toxicity concerns and limit suitability for biomedical applications,[19,216] while poor control over size, shape, and surface chemistry continues to limit reproducibility and targeted functionality.[217] Magnetic nanoparticle synthesis exemplifies these challenges, as hazardous multistep methods, difficulties in reducing poorly soluble oxides, aggregation, and reduced Curie temperatures compromise reproducibility and nanoscale stability.[218] Similarly, AgNP synthesis suffers from agglomeration, contamination, and poor stability, reducing antimicrobial activity.[29] For magnetic framework composites, limited studies and scarce biomedical evaluations further restrict comprehensive assessment of their potential.[19] Strontium-based semiconductors also remain hindered by low precursor solubility and stable adduct formation, which compromise their targeted electronic properties.[69] Highly soluble oxides such as B_2O_3 require sublimation or physical separation techniques due to poor by-product removal using conventional washing.[219] More broadly, end products are frequently contaminated by milling media, jars, or container abrasion,[181,220] which, alongside difficulties in tuning porosity, morphology, and uniformity, restricts the optimization of functional interfaces.

From a processing perspective, power ball milling has been widely employed for iron oxide synthesis,[221] yet limitations in particle size control, post-processing, and contamination remain acute. Even in successful demonstrations, such as magnetite nanoparticle synthesis *via* prolonged milling,[222] metallic impurities persisted. Knowledge on salt precursor reduction into noble metal nanoparticles remains scarce,[33] and diffusion-limited mass transfer further constrains reproducibility. Moreover, mechanochemical grafting often leads to reduced surface area, pore diameter, and pore volume, while increasing silane loadings diminish silylation efficiency and limit uniform functionalization.[8] Although polymer mechanochemistry holds promise, its extension to regulate heterogeneous catalysis a domain critical for industrial relevance has not yet been realized.[223]

Scaling laboratory processes to industrial production introduces further complexities. High-energy milling requires extensive optimization to balance quality, efficiency, and safety, while uncontrolled variables such as dust generation, noise, and equipment hazards demand stringent safety protocols.[144] The energy-intensive nature of high mechanical forces also raises concerns over sustainability, operational costs, and environmental impact when reliant on non-renewable sources.[215] Although mechanochemistry has advanced industrial use in pigmentation,[224] catalysis,[225] and wastewater treatment,[226] its broader adoption remains limited. Moreover, systematic evaluation using sustainability metrics such as atom economy and waste reduction remains underutilized, with only a few applications in MOFs and nanoparticles.[35] From a pharmaceutical manufacturing perspective, GMP compatibility of mechanochemical processes is platform-dependent. Continuous technologies, particularly twin-screw extrusion, are inherently more GMP-aligned due to enclosed operation, improved process control, and established pharmaceutical validation, whereas batch ball milling remains challenged by contamination risks and batch-to-batch variability, motivating a shift toward inert, enclosed, and continuous or hybrid reactors.

Taken together, these limitations underscore the dual challenge mechanochemistry faces: fundamental gaps in understanding multiscale reaction pathways[227] and practical obstacles in reproducibility, scalability, and interface tuning. Without bridging the divide between atomic-scale mechanisms and process-level control, the full potential of mechanochemical architectonics in constructing smart and functional interfaces will remain unrealized.

6.2. Future opportunities

Mechanochemistry offers a scalable, solvent-free, and energy-efficient platform to design advanced nanomaterials,

presenting significant opportunities for sustainable catalytic technologies beyond the limitations of conventional synthesis.[16] Expanding mechanochemistry into green and sustainable domains offers promising avenues to replace hazardous reagents, valorize biomass, and reduce energy inputs across inorganic material synthesis.[35] In this context, future strategies envision the integration of renewable feedstocks, such as biomass-derived reducing agents or plant extracts, to fabricate nanomaterials with enhanced catalytic performance, antimicrobial activity, and improved environmental compatibility.[29,228,229] Impressively, the material cost of this mechanochemical method has been reported to be less than 5% of those prepared using conventional sol–gel techniques,[230] highlighting its economic advantage. Mechanochemistry thus offers significant opportunities for producing nanoparticles from renewable and low-cost precursors while minimizing toxic chemicals and energy use.[231]

The future of mechanochemical research will also benefit from hybrid strategies that couple mechanical energy with thermal, light-based, or electromagnetic inputs, thereby enabling greater control over nanostructure formation and reaction selectivity.[159] Similarly, integrating mechanochemical methods with colloidal synthesis holds promise for overcoming current shape-control limitations, particularly in noble metal nanostructures, where anisotropy and tunability are crucial for applications in catalysis, sensing, and biomedicine.[33,232] The next phase of research should therefore prioritize precise size, shape, and composition control during synthesis, supported by deeper investigation into parameters such as ball-to-powder ratio, milling time, and post-milling heat treatments, including the influence of salt matrices and ion–surface interactions.[34,39,233] Developing strategies for soft-mechanochemical processing remains particularly critical for controlling size, shape, and agglomeration compared with more established non-soft approaches.[39]

In parallel with these broader technological advances, mechanochemistry enables clearly defined opportunities in nanomedicine and hybrid architectures. Force-driven synthesis supports solvent-free fabrication of inorganic–organic and biohybrid interfaces with enhanced stability, defect-mediated bioactivity, and controlled surface chemistry, enabling systematic development of multimodal bioimaging platforms, therapeutic nanozymes, and adaptive biomedical interfaces.

Beyond nanoparticles, mechanochemistry provides outstanding opportunities to access stoichiometric variations of inorganic compounds and synthesize ordered frameworks such as MOFs with tunable porosity, thereby advancing crystal engineering, adsorption, and separation technologies.[97,234,235] Mechanochemical methodologies have also demonstrated the ability to generate inorganic complexes and reactive species inaccessible by solution routes, with notable examples including kilogram-scale synthesis of Al(III) and In(III) salen and salophen complexes, which underscores the potential for industrial upscaling.[13,14] Such approaches can dramatically reduce reaction times from days to minutes, further enhancing energy efficiency for complex main-group and transition-metal compounds.[236] Recent advances in solvent-free C–C and C–N couplings exemplify how mechanochemistry can reshape sustainable industrial and pharmaceutical production,[69] while the growing exploration of bioconjugates involving proteins and monosaccharides points to future applications in supramolecular assembly and biointerfaces.[237]

The integration of real-time *in situ* monitoring with computational modeling, coupled with advanced synchrotron X-ray diffraction and Raman spectroscopy, provides new opportunities to unravel mechanochemical mechanisms with unprecedented resolution.[35,227] Such efforts will be complemented by the emerging concept of reversible mechanochemical reactions, which enables the exploration of equilibrium processes under mechanically driven conditions.[238] Life cycle assessment methodologies tailored to mechanochemistry offer a further opportunity to benchmark environmental performance against conventional routes, facilitating industrial adoption.[239] At the same time, advancing theoretical models and simulations to describe mass and energy transfer across different scales remains a pressing need for bridging laboratory insights with industrial process design.[240] Critically, the industrial translation of mechanochemistry requires optimization of equipment design, milling rates, and energy inputs, ensuring scalability while maintaining sustainability advantages.[144,241,242] Mechanochemical routes have already demonstrated significant potential to scale catalyst synthesis toward industrial levels while simultaneously reducing hazardous waste generation and energy consumption.[242] Future studies should therefore exploit mechanochemistry to design nanostructured catalysts with enhanced stability and selectivity, enabling applications in renewable energy and environmental remediation beyond traditional chemical production.[144,181] The emerging practice of integrating mechanochemistry with complementary electrochemical and photochemical methods further expands the scope of multifunctional pathways, opening new directions for energy storage, conversion, and sustainable environmental technologies.[144,243]

Altogether, these opportunities establish mechanochemistry not merely as a cost-effective and sustainable synthetic tool, but as a transformative paradigm for designing multiscale inorganic architectures and smart functional interfaces. By uniting green chemistry, computational modeling, real-time monitoring, and hybrid processing strategies, mechanochemistry is poised to shape the next generation of advanced nanomaterials with unprecedented precision, functionality, and scalability.

7. Conclusion

Mechanochemistry has evolved into a transformative paradigm in the synthesis of inorganic nanomaterials, enabling the deliberate construction of smart and functional interfaces through scalable, solvent-free, and energy-efficient routes. This review has articulated the conceptual foundation of mechanochemical architectonics, wherein mechanical force serves not merely as an energetic input but as a precise design parameter that orchestrates structural, interfacial, and functional evolution across multiple length scales. By bridging top-down comminution with bottom-up assembly, mechanochemical platforms ranging from ball milling and extrusion to hybrid

force-coupled strategies unlock reaction pathways inaccessible *via* conventional methods, fostering defect engineering, dynamic interface regeneration, and the creation of responsive nanostructures.

Case studies spanning catalysis, energy systems, biomedicine, and electronics affirm mechanochemistry's potential to deliver application-specific nanomaterials with superior performance, tunability, and sustainability. Nonetheless, challenges persist in achieving reproducibility, real-time mechanistic insight, and precise control over size, composition, and morphology. Future progress will hinge on integrating *in situ* diagnostics, multiscale computational modeling, and AI-guided synthesis to establish predictive control. Furthermore, coupling mechanochemical methods with electrochemical, photochemical, and bioinspired pathways promises to expand functionality while adhering to principles of green chemistry. Altogether, mechanochemical architectonics emerges not merely as a synthetic strategy but as a forward-looking materials design philosophy, poised to shape the next generation of inorganic nanotechnologies for sustainable and multifunctional applications.

Conflicts of interest

There are no conflicts of interest.

Abbreviations

AI	Artificial Intelligence
ANNs	Artificial Neural Networks
BPR	Ball-to-Powder Ratio
CoGEF	Constrained Geometries Simulate External Force
DEM	Discrete Element Method
DFT	Density Functional Theory
GO	Graphene Oxide
HER	Hydrogen Evolution Reaction
HKUST	Hong Kong University of Science and Technology (MOF family)
LAG	Liquid-Assisted Grinding
MOFs	Metal–Organic Frameworks
MXenes	Two-Dimensional Transition Metal Carbides/Nitrides
NMR	Nuclear Magnetic Resonance
NR	Nanorods
PAD	Push–Pull Protonated Atomic Distance
PLA	Polylactic Acid
PVA	Polyvinyl Alcohol
ROS	Reactive Oxygen Species
TSE	Twin-Screw Extrusion
WC	Tungsten Carbide

Data availability

No new data were generated or analyzed in this study. Data sharing is not applicable to this article as it is a review of previously published literature.

Supplementary information (SI) is available. See DOI: https://doi.org/10.1039/d5mr00116a.

Acknowledgements

This work was supported by a Universiti Sains Malaysia, Bridging Grant with Project No.: R501-LR-RND003-0000002097-0000.

References

1 A. D. McNaught and A. D. McNaught, *Compendium of Chemical Terminology*, Blackwell Science Oxford, vol. 1669, 1997.
2 P. Baláž, *et al.*, Hallmarks of mechanochemistry: from nanoparticles to technology, *Chem. Soc. Rev.*, 2013, **42**(18), 7571–7637.
3 L. Takacs, M. Carey Lea, the first mechanochemist, *J. Mater. Sci.*, 2004, **39**(16), 4987–4993.
4 D. E. Crawford, *et al.*, Organic synthesis by Twin Screw Extrusion (TSE): continuous, scalable and solvent-free, *Green Chem.*, 2017, **19**(6), 1507–1518.
5 D. Crawford, *et al.*, Synthesis by extrusion: continuous, large-scale preparation of MOFs using little or no solvent, *Chem. Sci.*, 2015, **6**(3), 1645–1649.
6 T. Auvray and T. Friščić, Shaking things from the ground-up: A systematic overview of the mechanochemistry of hard and high-melting inorganic materials, *Molecules*, 2023, **28**(2), 897.
7 N. Celik, *et al.*, Mechanochemical coupling of alkylsilanes to nanoparticles for solvent-free and rapid fabrication of superhydrophobic materials, *ACS Appl. Nano Mater.*, 2023, **6**(16), 14921–14930.
8 A. P. Amrute, B. Zibrowius and F. Schüth, Mechanochemical grafting: A solvent-less highly efficient method for the synthesis of hybrid inorganic–organic materials, *Chem. Mater.*, 2020, **32**(11), 4699–4706.
9 C. Suryanarayana, Mechanical alloying and milling, *Prog. Mater Sci.*, 2001, **46**(1–2), 1–184.
10 L. Russo, *et al.*, A mechanochemical approach to porous silicon nanoparticles fabrication, *Materials*, 2011, **4**(6), 1023–1033.
11 M. J. Rak, *et al.*, Mechanosynthesis of ultra-small monodisperse amine-stabilized gold nanoparticles with controllable size, *Green Chem.*, 2014, **16**(1), 86–89.
12 G. Karagedov and N. Lyakhov, Mechanochemical grinding of inorganic oxides, *Kona Powder Part. J.*, 2003, **21**, 76–87.
13 M. J. Rak, T. Friščić and A. Moores, Mechanochemical synthesis of Au, Pd, Ru and Re nanoparticles with lignin as a bio-based reducing agent and stabilizing matrix, *Faraday Discuss.*, 2014, **170**, 155–167.
14 V. Šepelák, *et al.*, High-resolution 27Al MAS NMR spectroscopic studies of the response of spinel aluminates to mechanical action, *J. Mater. Chem.*, 2011, **21**(23), 8332–8337.
15 K. Ralphs, C. Hardacre and S. L. James, Application of heterogeneous catalysts prepared by mechanochemical synthesis, *Chem. Soc. Rev.*, 2013, **42**(18), 7701–7718.
16 C. Xu, *et al.*, Mechanochemical synthesis of advanced nanomaterials for catalytic applications, *Chem. Commun.*, 2015, **51**(31), 6698–6713.

17 T. Tsuzuki and P. G. McCormick, Mechanochemical synthesis of nanoparticles, *J. Mater. Sci.*, 2004, **39**(16), 5143–5146.
18 F. Gomollón-Bel, Ten Chemical Innovations That Will Change Our World: IUPAC identifies emerging technologies in Chemistry with potential to make our planet more sustainable, *Chem. Int.*, 2019, **41**(2), 12–17.
19 M. Bellusci, *et al.*, Magnetic metal–organic framework composite by fast and facile mechanochemical process, *Inorg. Chem.*, 2018, **57**(4), 1806–1814.
20 S. Kumar, *et al.*, All-inorganic CsPbBr3 nanocrystals: gram-scale mechanochemical synthesis and selective photocatalytic CO2 reduction to methane, *ACS Appl. Energy Mater.*, 2020, **3**(5), 4509–4522.
21 Y. Sun, *et al.*, Synthesis and formation mechanism of cubic ZrN nanopowders by mechanochemical reaction of ZrCl4 and Li3N, *J. Alloys Compd.*, 2009, **479**(1–2), 599–602.
22 R. N. Baig and R. S. Varma, Alternative energy input: mechanochemical, microwave and ultrasound-assisted organic synthesis, *Chem. Soc. Rev.*, 2012, **41**(4), 1559–1584.
23 J.-L. Do and T. Friščić, Mechanochemistry: a force of synthesis, *ACS Cent. Sci.*, 2017, **3**(1), 13–19.
24 B. G. Fiss, *et al.*, Solvent-free mechanochemical synthesis of ultrasmall nickel phosphide nanoparticles and their application as a catalyst for the hydrogen evolution reaction (HER), *ACS Sustain. Chem. Eng.*, 2020, **8**(32), 12014–12024.
25 A. Vílchez, *et al.*, Mechanochemical synthesis of TiO2 nanoparticles and their self-organization at interfaces to produce emulsion-templated photocatalytic porous polymers, *J. Inorg. Organomet. Polym. Mater.*, 2021, **31**(5), 1912–1930.
26 J. Chen, K. Shen and Y. Li, Greening the processes of metal–organic framework synthesis and their use in sustainable catalysis, *ChemSusChem*, 2017, **10**(16), 3165–3187.
27 J. Andersen and J. Mack, Mechanochemistry and organic synthesis: from mystical to practical, *Green Chem.*, 2018, **20**(7), 1435–1443.
28 T. D. Isfahani, *et al.*, Mechanochemical synthesis of zirconia nanoparticles: Formation mechanism and phase transformation, *Int. J. Refract. Met. Hard Mater.*, 2012, **31**, 21–27.
29 M. Kováčová, *et al.*, Sustainable one-step solid-state synthesis of antibacterially active silver nanoparticles using mechanochemistry, *Nanomaterials*, 2020, **10**(11), 2119.
30 D. Becker, M. Klos and G. Kickelbick, Mechanochemical synthesis of Mn3O4 nanocrystals and their lithium intercalation capability, *Inorg. Chem.*, 2019, **58**(22), 15021–15024.
31 S. L. James, *et al.*, Mechanochemistry: opportunities for new and cleaner synthesis, *Chem. Soc. Rev.*, 2012, **41**(1), 413–447.
32 O. Lapshin, E. Boldyreva and V. Boldyrev, Role of mixing and milling in mechanochemical synthesis, *Russ. J. Inorg. Chem.*, 2021, **66**(3), 433–453.
33 P. F. de Oliveira, *et al.*, Challenges and opportunities in the bottom-up mechanochemical synthesis of noble metal nanoparticles, *J. Mater. Chem. A*, 2020, **8**(32), 16114–16141.
34 Y. Xia, *et al.*, Shape-controlled synthesis of metal nanocrystals: simple chemistry meets complex physics?, *Angew. Chem., Int. Ed.*, 2009, **48**(1), 60–103.
35 B. G. Fiss, *et al.*, Mechanochemical methods for the transfer of electrons and exchange of ions: inorganic reactivity from nanoparticles to organometallics, *Chem. Soc. Rev.*, 2021, **50**(14), 8279–8318.
36 F. Cuccu, *et al.*, Mechanochemistry: New Tools to Navigate the Uncharted Territory of "Impossible" Reactions, *ChemSusChem*, 2022, **15**(17), e202200362.
37 D. Singh and S. Dilip Saoji, Nanoarchitectonics in Macromolecular Science: Integrating Molecular Dynamics with Smart Materials, *J. Macromol. Sci., Part B: Phys.*, 2024, 1–10.
38 T. Tsuzuki, Mechanochemical synthesis of metal oxide nanoparticles, *Commun. Chem.*, 2021, **4**, 143, DOI: 10.1038/s42004-021-00582-3.
39 T. Tsuzuki, Mechanochemical synthesis of metal oxide nanoparticles, *Commun. Chem.*, 2021, **4**(1), 143.
40 J. N. Stevanović, *et al.*, Mechanochemical Synthesis of TiO(2)-CeO(2) Mixed Oxides Utilized as a Screen-Printed Sensing Material for Oxygen Sensor, *Sensors*, 2023, **23**(3), 1313.
41 Q. Shi, *et al.*, Nano-architectonics of Pt single-atoms and differently-sized nanoparticles supported by manganese-oxide nanosheets and impact on catalytic and anti-biofilm activities, *J. Colloid Interface Sci.*, 2024, **672**, 224–235.
42 E. Colacino, F. Delogu and T. Hanusa, Advances in Mechanochemistry, *ACS Sustain. Chem. Eng.*, 2021, **9**(32), 10662–10663.
43 X. Liu, *et al.*, A review on mechanochemistry: approaching advanced energy materials with greener force, *Adv. Mater.*, 2022, **34**(46), 2108327.
44 J.-L. Do and T. Friščić, Mechanochemistry: A Force of Synthesis, *ACS Cent. Sci.*, 2017, **3**(1), 13–19.
45 P. F. M. de Oliveira, *et al.*, Challenges and opportunities in the bottom-up mechanochemical synthesis of noble metal nanoparticles, *J. Mater. Chem. A*, 2020, **8**(32), 16114–16141.
46 J. Beamish-Cook, *et al.*, Insights into the Mechanochemical Synthesis of MOF-74, *Cryst. Growth Des.*, 2021, **21**(5), 3047–3055.
47 M. Klimakow, *et al.*, Mechanochemical Synthesis of Metal−Organic Frameworks: A Fast and Facile Approach toward Quantitative Yields and High Specific Surface Areas, *Chem. Mater.*, 2010, **22**(18), 5216–5221.
48 G.-Y. Yan, *et al.*, Mechanochemical solid state architectonics on Lead(II) coordination polymer by anion-exchange, *J. Solid State Chem.*, 2021, **304**, 122592.
49 M. Avinash and T. Govindaraju, Architectonics: design of molecular architecture for functional applications, *Acc. Chem. Res.*, 2018, **51**(2), 414–426.
50 R. Huang, *et al.*, Molecular design and architectonics towards film-based fluorescent sensing, *Chem. Soc. Rev.*, 2024, **53**(13), 6960–6991.

51 L. Dong, *et al.*, Mechanochemistry: Fundamental Principles and Applications, *Adv. Sci.*, 2025, **12**(24), 2403949.
52 S. Hwang, S. Grätz and L. Borchardt, A guide to direct mechanocatalysis, *Chem. Commun.*, 2022, **58**(11), 1661–1671.
53 T. Stauch and A. Dreuw, Advances in quantum mechanochemistry: electronic structure methods and force analysis, *Chem. Rev.*, 2016, **116**(22), 14137–14180.
54 M. Zakeri, M. Ramezani and A. Nazari, Effect of ball to powder weight ratio on the mechanochemical synthesis of MoSi2-TiC nanocomposite powder, *Mater. Res.*, 2012, **15**, 891–897.
55 A. M. Belenguer, G. I. Lampronti and J. K. M. Sanders, Reliable Mechanochemistry: Protocols for Reproducible Outcomes of Neat and Liquid Assisted Ball-mill Grinding Experiments, *J. Visualized Exp.*, 2018, **131**, 56824.
56 O. F. Jafter, *et al.*, Navigating Ball Mill Specifications for Theory-to-Practice Reproducibility in Mechanochemistry, *Angew. Chem., Int. Ed.*, 2024, **63**(48), e202409731.
57 L. K. Wei, *et al.*, Producing Metal Powder from Machining Chips Using Ball Milling Process: A Review, *Materials*, 2023, **16**(13), 4635.
58 R. De Armas, M. Temprado and L. M. Frutos, Computational Model to Predict Reactivity under Ball-Milling Conditions, *J. Chem. Theory Comput.*, 2025, **21**(20), 10353–10361.
59 A. Krusenbaum, *et al.*, The mechanochemical synthesis of polymers, *Chem. Soc. Rev.*, 2022, **51**(7), 2873–2905.
60 A. Ochirkhuyag, *et al.*, One-pot mechanochemical ball milling synthesis of the MnOx nanostructures as efficient catalysts for CO2 hydrogenation reactions, *Phys. Chem. Chem. Phys.*, 2020, **22**(25), 13999–14012.
61 B. Zhao, *et al.*, Multifunctional Iron Oxide Nanoflake/Graphene Composites Derived from Mechanochemical Synthesis for Enhanced Lithium Storage and Electrocatalysis, *ACS Appl. Mater. Interfaces*, 2015, **7**(26), 14446–14455.
62 G. Bharath, *et al.*, Solvent-free mechanochemical synthesis of graphene oxide and Fe3O4–reduced graphene oxide nanocomposites for sensitive detection of nitrite, *J. Mater. Chem. A*, 2015, **3**(30), 15529–15539.
63 W. Xiao, *et al.*, Facile Synthesis of Highly Porous Metal Oxides by Mechanochemical Nanocasting, *Chem. Mater.*, 2018, **30**(9), 2924–2929.
64 V. Oskoei, M. Mathesh and W. Yang, Mechanochemical Nanoarchitectonics for the Synthesis of Enzyme-Based Hydrogen-Bonded Organic Frameworks, *Chem. Mater.*, 2025, **37**(18), 7206–7213.
65 R. Li, *et al.*, Mechanochemical Synthesis of Defective Molybdenum Trioxide, Titanium Dioxide, and Zinc Oxide at Room Temperature, *ACS Sustain. Chem. Eng.*, 2019, **7**(14), 11985–11989.
66 A. D. Katsenis, *et al.*, In situ X-ray diffraction monitoring of a mechanochemical reaction reveals a unique topology metal-organic framework, *Nat. Commun.*, 2015, **6**(1), 6662.
67 H. Kulla, *et al.*, In Situ Investigations of Mechanochemical One-Pot Syntheses, *Angew Chem. Int. Ed. Engl.*, 2018, **57**(20), 5930–5933.
68 G. Zhang, *et al.*, Fabrication of MBene-Based ZIF Flame Retardant Epoxy Resin via Green and Feasible Mechanochemical Method, *ACS Sustain. Chem. Eng.*, 2025, **13**(27), 10573–10586.
69 J. F. Reynes, F. Leon and F. García, Mechanochemistry for organic and inorganic synthesis, *ACS Org. Inorg. Au*, 2024, **4**(5), 432–470.
70 D. Sarmah, A. Hazarika and B. K. Saikia, Graphene Architectures in Coal-Derived Carbon: Turbostratic Twist and Supercapacitor Promise, *Energy Fuels*, 2025, **39**(30), 14724–14737.
71 V. Boldyrev and K. Tkáčová, Mechanochemistry of solids: past, present, and prospects, *J. Mater. Synth. Process.*, 2000, **8**(3), 121–132.
72 T. Friščić, C. Mottillo and H. M. Titi, Mechanochemistry for synthesis, *Angew. Chem.*, 2020, **132**(3), 1030–1041.
73 L. Takacs, The historical development of mechanochemistry, *Chem. Soc. Rev.*, 2013, **42**(18), 7649–7659.
74 C. G. Vogt, *et al.*, Bronze age of direct mechanocatalysis: how alloyed milling materials advance coupling in ball mills, *Adv. Energy Sustainability Res.*, 2021, **2**(5), 2100011.
75 P. A. Julien and T. Friscic, Methods for monitoring milling reactions and mechanistic studies of mechanochemistry: a primer, *Cryst. Growth Des.*, 2022, **22**(9), 5726–5754.
76 J. Mack, *et al.*, The first solvent-free method for the reduction of esters, *Green Chem.*, 2007, **9**(10), 1041–1043.
77 Y. Gao, K. Kubota and H. Ito, Mechanochemical Approach for Air-Tolerant and Extremely Fast Lithium-Based Birch Reductions in Minutes, *Angew. Chem.*, 2023, **135**(21), e202217723.
78 H. U. Escobar-Hernandez, *et al.*, Life cycle assessment of metal–organic frameworks: sustainability study of zeolitic imidazolate framework-67, *ACS Sustain. Chem. Eng.*, 2023, **11**(10), 4219–4225.
79 Y. Lou, *et al.*, Mechanochemical Urea Synthesis Using Ammonia–Water and Carbon Dioxide Under Mild Conditions: An Experimental and Theoretical Study, *ACS Sustain. Chem. Eng.*, 2025, **13**(1), 151–164.
80 B. Dhokale, *et al.*, Mechanochemistry for the Sustainable Synthesis of Organic Hole Transport Materials in Perovskite Solar Cells, *Cryst. Growth Des.*, 2025, **25**(8), 2402–2408.
81 E. Marín, X. Vendrell and J. Llorca, Pd Supported on CeO2 Nanostructures Prepared by Planetary Ball Milling under a Modified Atmosphere for Catalytic Oxidation of CO, *ACS Appl. Nano Mater.*, 2025, **8**(23), 12151–12163.
82 X. Shen, *et al.*, Rapid mechanochemical synthesis of polyanionic cathode with improved electrochemical performance for Na-ion batteries, *Nat. Commun.*, 2021, **12**(1), 2848.
83 R. Schlem, *et al.*, Energy storage materials for solid-state batteries: design by mechanochemistry, *Adv. Energy Mater.*, 2021, **11**(30), 2101022.
84 S. He, *et al.*, Solvent-free mechanochemical synthesis of Na-rich Prussian white cathodes for high-performance Na-ion batteries, *Chem. Eng. J.*, 2022, **428**, 131083.
85 G. Liu, *et al.*, High air-stability and superior lithium ion conduction of Li3+ 3xP1-xZnxS4-xOx by aliovalent

substitution of ZnO for all-solid-state lithium batteries, *Energy Storage Mater.*, 2019, **17**, 266–274.
86 B. Biswas, *et al.*, Mechanochemically Activated Halloysite Nanotube-Rich Kaolin Clay As a Carrier for Slow-Release Phosphate Fertilizer, *ACS Sustain. Chem. Eng.*, 2025, **13**(23), 8711–8721.
87 W. Cai, *et al.*, Mechanochemically Driven C–C Bond Formation via Cu-Complex-Functionalized Polyoxoniobate under Solvent-Free Conditions, *Cryst. Growth Des.*, 2025, **25**(5), 1636–1643.
88 I. Sande, *et al.*, Mechanochemical Synthesis of 2-Amino-1, 4-naphthoquinones and Telescopic Synthesis of Lawsone, *ACS Omega*, 2025, **10**(40), 46369–46383.
89 T. Plant-Collins, *et al.*, Beyond Solution Chemistry: Mechanochemistry Enables Clustered Defects in Metal–Organic Frameworks, *Inorg. Chem.*, 2025, **64**(34), 17436–17447.
90 S. L. James and T. Friščić, Mechanochemistry, *Chem. Soc. Rev.*, 2013, **42**(18), 7494–7496.
91 T. Friščić, *et al.*, Ion-and liquid-assisted grinding: improved mechanochemical synthesis of metal–organic frameworks reveals salt inclusion and anion templating, *Angew. Chem., Int. Ed.*, 2010, **49**(4), 712–715.
92 Y. Filinchuk, *et al.*, Porous and dense magnesium borohydride frameworks: synthesis, stability, and reversible absorption of guest species, *Angew. Chem.*, 2011, **123**(47), 11358–11362.
93 R. Zhou, *et al.*, Cu-MOF@ Pt 3D nanocomposites prepared by one-step wrapping method with peroxidase-like activity for colorimetric detection of glucose, *Colloids Surf., B*, 2022, **216**, 112601.
94 J. Alić, *et al.*, Meeting the UN sustainable development goals with mechanochemistry, *Angew. Chem., Int. Ed.*, 2024, **63**(50), e202414745.
95 M. Mohamed, *et al.*, Mechanochemical synthesis of Li-rich (Li 2 Fe) SO cathode for Li-ion batteries, *Green Chem.*, 2023, **25**(10), 3878–3887.
96 G.-F. Han, *et al.*, Mechanochemistry for ammonia synthesis under mild conditions, *Nat. Nanotechnol.*, 2021, **16**(3), 325–330.
97 S. Głowniak, *et al.*, Mechanochemistry: Toward green synthesis of metal–organic frameworks, *Mater. Today*, 2021, **46**, 109–124.
98 A. M. Fidelli, *et al.*, Green and rapid mechanosynthesis of high-porosity NU-and UiO-type metal–organic frameworks, *Chem. Commun.*, 2018, **54**(51), 6999–7002.
99 S. Bonciolini, A. Pulcinella and T. Noël, Tech-Enhanced Synthesis: Exploring the Synergy between Organic Chemistry and Technology, *J. Am. Chem. Soc.*, 2025, **147**(32), 28523–28545.
100 D. E. Crawford, *et al.*, Solvent-free, continuous synthesis of hydrazone-based active pharmaceutical ingredients by twin-screw extrusion, *ACS Sustain. Chem. Eng.*, 2020, **8**(32), 12230–12238.
101 M. Lavayssiere and F. Lamaty, Amidation by reactive extrusion for the synthesis of active pharmaceutical ingredients teriflunomide and moclobemide, *Chem. Commun.*, 2023, **59**(23), 3439–3442.
102 R. R. Bolt, *et al.*, Solvent Minimized Synthesis of Amides by Reactive Extrusion, *Angew. Chem.*, 2024, **136**(41), e202408315.
103 Y. Song, *et al.*, Continuous and Large-Scale Preparation of Hierarchical Porous HKUST-1 via the "Nanofusion" Mechanism Using Liquid-Assisted Mechanosynthesis, *Inorg. Chem.*, 2025, **64**(11), 5579–5585.
104 Y. Xie, *et al.*, Hygroscopicity Reduction and Interconversion of Ligustrazine in Ligusticum chuanxiong Hort. via Cocrystallization and Mechanochemical Technology, *Cryst. Growth Des.*, 2025, **25**(16), 6686–6696.
105 J. Wang, *et al.*, Self-Correcting Assembly via Mechanochemical Polymer Rearrangement for Scalable Nanostructure Manufacturing, *ACS Mater. Lett.*, 2024, **6**(10), 4443–4451.
106 S. Zeng, *et al.*, Green Preparation of High-Performance Poly (Vinyl Alcohol) Film by Combining Gel-Like Extrusion and Biaxial Stretching, *Ind. Eng. Chem. Res.*, 2024, **63**(19), 8622–8632.
107 N. Kurbanova, S. Ragimova and T. Guliyeva, Nickel-Containing Nanocomposites Based on Isotactic Polypropylene and High-Pressure Polyethylene, *Inorg. Mater. Appl. Res.*, 2024, **15**(5), 1350–1354.
108 C. Pina-Vidal, *et al.*, Mechanochemical encapsulation of caffeine in UiO-66 and UiO-66-NH2 to obtain polymeric composites by extrusion with recycled polyamide 6 or polylactic acid biopolymer, *Polymers*, 2024, **16**(5), 637.
109 B. A. Steele, *et al.*, Mechanochemical synthesis of glycine oligomers in a virtual rotational diamond anvil cell, *Chem. Sci.*, 2020, **11**(30), 7760–7771.
110 J. A. Ciezak-Jenkins and T. A. Jenkins, Mechanochemical induced structural changes in sucrose using the rotational diamond anvil cell, *J. Appl. Phys.*, 2018, **123**(8), 085901.
111 G. De Bo, Mechanochemistry of the mechanical bond, *Chem. Sci.*, 2018, **9**(1), 15–21.
112 H. Yan, *et al.*, Sterically controlled mechanochemistry under hydrostatic pressure, *Nature*, 2018, **554**(7693), 505–510.
113 L. Zhu, *et al.*, Mechanochemistry, solvent-free and scale-up: Application toward coupling of acids and amines to amides, *Results Chem.*, 2023, **5**, 100882.
114 C. Espro and D. Rodriguez-Padron, Re-thinking organic synthesis: Mechanochemistry as a greener approach, *Curr. Opin. Green Sustainable Chem.*, 2021, **30**, 100478.
115 B. Cecen, *et al.*, Smart biomaterials in biomedical applications: current advances and possible future directions, *Macromol. Biosci.*, 2024, **24**(3), 2200550.
116 S. Iravani, *et al.*, Advancements in MXenes and mechanochemistry: exploring new horizons and future applications, *Mater. Adv.*, 2024, **5**(21), 8404–8418.
117 V. Martinez, *et al.*, Advancing mechanochemical synthesis by combining milling with different energy sources, *Nat. Rev. Chem.*, 2023, **7**(1), 51–65.
118 X. Wang, *et al.*, Defect Engineering to Boost the Lithium-Ion Storage Performance of Ti3C2T x MXene Induced by

Plasma-Assisted Mechanochemistry, *ACS Appl. Energy Mater.*, 2021, **4**(9), 10280–10289.
119 J. Wang, *et al.*, Mechanochemistry-induced biaxial compressive strain engineering in MXenes for boosting lithium storage kinetics, *Nano Energy*, 2021, **87**, 106053.
120 S. Zhang, *et al.*, An MXene/CNTs@ P nanohybrid with stable Ti–O–P bonds for enhanced lithium ion storage, *J. Mater. Chem. A*, 2019, **7**(38), 21766–21773.
121 X. Liu, *et al.*, Solid-state mechanochemistry advancing two dimensional materials for lithium-ion storage applications: A mini review, *Nano Mater. Sci.*, 2023, **5**(2), 210–227.
122 J. Batteas, *et al.*, Moving mechanochemistry forward, *RSC Mechanochem.*, 2025, **2**(1), 10–19.
123 M. Senna and A. A. Michalchuk, Reassessing mechanochemical processes in polyatomic systems for smart fabrication of nanocomposites, *RSC Mechanochem.*, 2025, **2**(3), 351–369.
124 W. A. Ali, S. E. Richards and R. H. Alzard, Unlocking the potential of ball milling for nanomaterial Synthesis: An overview, *J. Ind. Eng. Chem.*, 2025, **149**, 63–93.
125 S. W. Hwang, *et al.*, Hybrid Vesicles Enable Mechano-Responsive Hydrogel Degradation, *Angew. Chem.*, 2023, **135**(41), e202308509.
126 C. Wang, *et al.*, How external forces affect the degradation properties of perfluorooctanoic acid in mechanochemical degradation: a DFT study, *RSC Mechanochem.*, 2025, **2**, 692–705.
127 S. Mittal, *et al.*, Molecular dynamics model of mechanophore sensors for biological force measurement, *Heliyon*, 2025, **11**(1), e41178.
128 S. Ghose, *et al.*, Response of a Tethered Zn-Bis-Terpyridine Complex to an External Mechanical Force: A Computational Study of the Roles of the Tether and Solvent, *J. Phys. Chem. A*, 2025, **129**(15), 3423–3434.
129 X. Zhao, *et al.*, Hybrid Spike-Facilitated Capture and Biofilm Destruction Co-Enhances Ultrasound-Mediated Bactericidal Therapy, *ACS Nano*, 2025, **19**(35), 31720–31739.
130 J. Qu, *et al.*, Mechanochemically synthesised MXene@ PAbz hybrids endow EP coatings with excellent fire safety performance, *Chem. Eng. J.*, 2025, 167688.
131 M. Rok, *et al.*, Secret agent in the secret service: Utilization of Sb (iii)-based complexes' emission properties for the study of forgery and document authenticity, *J. Mater. Chem. C*, 2025, **13**(33), 17241–17250.
132 E. C. Spencer, *et al.*, Pressure-Induced Bond Rearrangement and Reversible Phase Transformation in a Metal–Organic Framework, *Angew. Chem.*, 2014, **126**(22), 5689–5692.
133 A. V. Neimark, *et al.*, Structural transitions in MIL-53 (Cr): view from outside and inside, *Langmuir*, 2011, **27**(8), 4734–4741.
134 T. D. Bennett, *et al.*, Reversible pressure-induced amorphization of a zeolitic imidazolate framework (ZIF-4), *Chem. Commun.*, 2011, **47**(28), 7983–7985.
135 A. U. Ortiz, *et al.*, Anisotropic Elastic Properties of Flexible Metal-Organic Frameworks:<? format?> How Soft are Soft Porous Crystals?, *Phys. Rev. Lett.*, 2012, **109**(19), 195502.
136 J. McCarron, B. Turner and L. N. McHugh, Hybrid Framework Materials: Next-Generation Engineering Materials, *Adv. Eng. Mater.*, 2025, **27**(9), 2402554.
137 E. C. Spencer, *et al.*, Pressure-induced cooperative bond rearrangement in a zinc imidazolate framework: a high-pressure single-crystal X-ray diffraction study, *J. Am. Chem. Soc.*, 2009, **131**(11), 4022–4026.
138 S. Henke, W. Li and A. K. Cheetham, Guest-dependent mechanical anisotropy in pillared-layered soft porous crystals–a nanoindentation study, *Chem. Sci.*, 2014, **5**(6), 2392–2397.
139 T. D. Bennett, *et al.*, Connecting defects and amorphization in UiO-66 and MIL-140 metal–organic frameworks: a combined experimental and computational study, *Phys. Chem. Chem. Phys.*, 2016, **18**(3), 2192–2201.
140 K. Uzarevic, I. Halasz and T. Friscic, Real-time and in situ monitoring of mechanochemical reactions: A new playground for all chemists, *J. Phys. Chem. Lett.*, 2015, **6**(20), 4129–4140.
141 W. Wang, *et al.*, Metal–organic framework composites from a mechanochemical process, *Mol. Syst. Des. Eng.*, 2023, **8**(5), 560–579.
142 E. Boldyreva, Mechanochemistry of inorganic and organic systems: what is similar, what is different?, *Chem. Soc. Rev.*, 2013, **42**(18), 7719–7738.
143 B. Szczęśniak, *et al.*, Mechanochemical synthesis of highly porous materials, *Mater. Horiz.*, 2020, **7**(6), 1457–1473.
144 A. B. Chetry, Mechanochemistry: A new frontier in chemical synthesis, *J. Chem. Res.*, 2025, **49**(3), 17475198251339299.
145 Y. Wu, K. Lin and J. Ruan, Control the Mechanochemical Energy of Ball Milling To Remove Surface Organic Contamination without Damaging the Integrity of the Glass, *ACS Sustain. Chem. Eng.*, 2023, **11**(41), 15083–15090.
146 Z. Yang, *et al.*, Chiral superstructures of inorganic nanorods by macroscopic mechanical grinding, *Nat. Commun.*, 2022, **13**(1), 5844.
147 S. Cao, *et al.*, Amorphization of the prototypical zeolitic imidazolate framework ZIF-8 by ball-milling, *Chem. Commun.*, 2012, **48**(63), 7805–7807.
148 M. Taheri, *et al.*, Green full conversion of ZnO nanopowders to well-dispersed zeolitic imidazolate framework-8 (ZIF-8) nanopowders via a stoichiometric mechanochemical reaction for fast dye adsorption, *Cryst. Growth Des.*, 2020, **20**(4), 2761–2773.
149 Y.-R. Miao and K. S. Suslick, Mechanochemical reactions of metal-organic frameworks, in *Advances in Inorganic Chemistry*, Elsevier, 2018, pp. 403–434.
150 S. Tanaka, *et al.*, Mechanochemical dry conversion of zinc oxide to zeolitic imidazolate framework, *Chem. Commun.*, 2013, **49**(72), 7884–7886.
151 V. Šepelák, S. Bégin-Colin and G. Le Caer, Transformations in oxides induced by high-energy ball-milling, *Dalton Trans.*, 2012, **41**(39), 11927–11948.
152 J. M. Marrett, *et al.*, Mechanochemistry for Metal–Organic Frameworks and Covalent–Organic Frameworks (MOFs, COFs): Methods, Materials, and Mechanisms, *Adv. Mater.*, 2025, 2418707.

153 X. Zhou, *et al.*, Mechanochemistry of metal–organic frameworks under pressure and shock, *Acc. Chem. Res.*, 2020, **53**(12), 2806–2815.
154 J. De Bellis, *et al.*, Surface and bulk chemistry of mechanochemically synthesized tohdite nanoparticles, *J. Am. Chem. Soc.*, 2022, **144**(21), 9421–9433.
155 X. Li, *et al.*, Mechanochemistry-assisted encapsulation of metal nanoparticles in MOF matrices via a sacrificial strategy, *J. Mater. Chem. A*, 2019, **7**(24), 14504–14509.
156 H. K. Lee, J. H. Lee and H. R. Moon, Mechanochemistry as a reconstruction tool of decomposed metal–organic frameworks, *Inorg. Chem.*, 2021, **60**(16), 11825–11829.
157 I. R. Speight and T. P. Hanusa, Exploration of mechanochemical activation in solid-state fluoro-Grignard reactions, *Molecules*, 2020, **25**(3), 570.
158 N. C. Boyde, *et al.*, Symmetric Assembly of a Sterically Encumbered Allyl Complex: Mechanochemical and Solution Synthesis of the Tris (Allyl) Beryllate, K [BeA′ 3](A′= 1, 3-(SiMe3) 2C3H3), *Inorganics*, 2017, **5**(2), 36.
159 H. Hasan, F. Arshad and M. P. Sk, Mechanochemical conversion of elemental sulfur into functional sulfur nanomaterials for promising applications, *RSC Mechanochem.*, 2025, **2**(6), 786–801.
160 H. Cheng, *et al.*, Mechanochemical synthesis of highly porous CeMnO x catalyst for the removal of NO x, *Ind. Eng. Chem. Res.*, 2019, **58**(36), 16472–16478.
161 B. Zhang, *et al.*, Embedding hierarchical pores by mechanochemistry in carbonates with superior chemoselective catalysis and stability, *Inorg. Chem.*, 2023, **62**(32), 12920–12930.
162 D. Yu, *et al.*, Alkali metals and cerium-modified La–Co-based perovskite catalysts: facile synthesis, excellent catalytic performance, and reaction mechanisms for soot combustion, *ACS Catal.*, 2022, **12**(24), 15056–15075.
163 G. I. Bell, Models for the specific adhesion of cells to cells: a theoretical framework for adhesion mediated by reversible bonds between cell surface molecules, *Science*, 1978, **200**(4342), 618–627.
164 N. Hopper, *et al.*, Exploring mechanochemical reactions at the nanoscale: Theory versus experiment, *Phys. Chem. Chem. Phys.*, 2023, **25**(23), 15855–15861.
165 R. Rana, *et al.*, Anisotropy of shear-induced mechanochemical reaction rates of surface adsorbates; implications for theoretical models, *J. Phys. Chem. C*, 2022, **126**(28), 11585–11593.
166 T. Bunno, *et al.*, Ternary Triazole-Based Organic–Inorganic Proton-Conducting Hybrids Based on Computational Models for HT-PEMFC Application, *ACS Omega*, 2023, **8**(46), 44172–44182.
167 T. Wu and J. Wang, Deep mining stable and nontoxic hybrid organic–inorganic perovskites for photovoltaics via progressive machine learning, *ACS Appl. Mater. Interfaces*, 2020, **12**(52), 57821–57831.
168 B. Chen, R. Hoffmann and R. Cammi, The effect of pressure on organic reactions in fluids—a new theoretical perspective, *Angew. Chem., Int. Ed.*, 2017, **56**(37), 11126–11142.
169 M. T. Ong, *et al.*, First principles dynamics and minimum energy pathways for mechanochemical ring opening of cyclobutene, *J. Am. Chem. Soc.*, 2009, **131**(18), 6377–6379.
170 W. Sakai, *et al.*, Origin of stereoselectivity in a mechanochemical reaction of diphenylfulvene and maleimide, *J. Phys. Chem. A*, 2023, **127**(28), 5790–5794.
171 B. S. Pladevall, A. de Aguirre and F. Maseras, Understanding ball milling mechanochemical processes with DFT calculations and microkinetic modeling, *ChemSusChem*, 2021, **14**(13), 2763–2768.
172 H. Rojas-Chávez, *et al.*, A Comparative DFT Study on Process Control Agents in the Mechanochemical Synthesis of PbTe, *Int. J. Mol. Sci.*, 2022, **23**(19), 11194.
173 H. Adams, Modeling mechanochemical reaction mechanisms, *ACS Appl. Mater. Interfaces*, 2017, **9**(31), 26531–26538.
174 M. Fusaro, *et al.*, Computational modeling of gold nanoparticle interacting with molecules of pharmaceutical interest in water, *Molecules*, 2023, **28**(20), 7167.
175 K. Triatmaja, *et al.*, Development of Graphene Oxide-Based Antibacterial Agents via ZnO/Eugenol Modification: Experimental and Computational Analysis, *Indones. J. Chem.*, 2025, **25**(2), 359.
176 L. Yang, *et al.*, Thermodynamics model for mechanochemical synthesis of gold nanoparticles: Implications for solvent-free nanoparticle production, *ACS Appl. Nano Mater.*, 2021, **4**(2), 1886–1897.
177 H. T. Ta, *et al.*, Ab initio informed machine learning potential for tribochemistry and mechanochemistry: Application for eco–friendly gallate lubricant additive, *Comput. Mater. Today*, 2024, **1**, 100005.
178 J. R. Gröls and B. Castro-Dominguez, Mechanochemical co-crystallization: Insights and predictions, *Comput. Chem. Eng.*, 2021, **153**, 107416.
179 R. Shaikh, S. Shirazian and G. M. Walker, Application of artificial neural network for prediction of particle size in pharmaceutical cocrystallization using mechanochemical synthesis, *Neural Comput. Appl.*, 2021, **33**(19), 12621–12640.
180 M. U. Rahman, *et al.*, Computational chemistry unveiled: a critical analysis of theoretical coordination chemistry and nanostructured materials, *Chem. Prod. Process Model.*, 2024, **19**(4), 473–515.
181 A. P. Amrute, *et al.*, Mechanochemical synthesis of catalytic materials, *Chem.–Eur. J.*, 2021, **27**(23), 6819–6847.
182 F. García, M. Senna and V. Šepelák, Moving mechanochemistry forward: reimagining inorganic chemistry through mechanochemistry, *RSC Mechanochem.*, 2025, **2**, 499–502.
183 K. M. Siniard, *et al.*, Precision structure engineering of high-entropy oxides under ambient conditions, *ACS Catal.*, 2024, **14**(19), 14807–14818.
184 L. Xiao, *et al.*, A novel, solvent-free mechanochemistry approach for gold extraction from anode slime, *ACS Sustain. Chem. Eng.*, 2019, **7**(13), 11415–11425.

185 W. Zhan, *et al.*, Incorporating rich mesoporosity into a ceria-based catalyst via mechanochemistry, *Chem. Mater.*, 2017, **29**(17), 7323–7329.
186 Q. Yang, *et al.*, Mechanochemistry Strategy in Metal/Fe3O4 with High Stability for Superior Chemoselective Catalysis, *ACS Appl. Mater. Interfaces*, 2024, **16**(48), 66219–66229.
187 W. Zhu, *et al.*, SupraCells: living mammalian cells protected within functional modular nanoparticle-based exoskeletons, *Adv. Mater.*, 2019, **31**(25), 1900545.
188 F. H. Silver, *Mechanosensing and Mechanochemical Transduction in Extracellular Matrix: Biological, Chemical, Engineering, and Physiological Aspects*, Springer, 2006.
189 P. Krupiński, *et al.*, From Uncommon Ethylzinc Complexes Supported by Ureate Ligands to Water-Soluble ZnO Nanocrystals: A Mechanochemical Approach, *ACS Sustain. Chem. Eng.*, 2021, **9**(4), 1540–1549.
190 Q. Ma, *et al.*, Solid SiO2-sealed mesoporous silica for synergistically combined use of inorganic and organic filters to achieve safe and effective skin protection from all-band UV radiation, *ACS Appl. Mater. Interfaces*, 2023, **15**(9), 12209–12220.
191 O. Mazaheri, *et al.*, Solid-state encapsulation of urea via mechanochemistry-driven engineering of metal–phenolic networks, *Chem. Mater.*, 2023, **35**(18), 7800–7813.
192 Q. Zhang, *et al.*, Zinc oxide nanorods for light-activated gas sensing and photocatalytic applications, *ACS Appl. Nano Mater.*, 2023, **6**(19), 17445–17456.
193 Y. Liu, *et al.*, Guest release from coordination assemblies in the solid state, *Chem*, 2024, **10**(5), 1502–1515.
194 L. Zheng, *et al.*, Unveiling the electronic interaction in ZnO/PtO/Pt nanoarrays for catalytic detection of triethylamine with ultrahigh sensitivity, *ACS Appl. Mater. Interfaces*, 2020, **12**(41), 46267–46276.
195 R. M. Dragoman, *et al.*, Surface-engineered cationic nanocrystals stable in biological buffers and high ionic strength solutions, *Chem. Mater.*, 2017, **29**(21), 9416–9428.
196 G. Zhang, *et al.*, Influence of anchoring ligands and particle size on the colloidal stability and in vivo biodistribution of polyethylene glycol-coated gold nanoparticles in tumor-xenografted mice, *Biomaterials*, 2009, **30**(10), 1928–1936.
197 R. Dubadi, S. D. Huang and M. Jaroniec, Mechanochemical synthesis of nanoparticles for potential antimicrobial applications, *Materials*, 2023, **16**(4), 1460.
198 H. Wang, *et al.*, Applications of metal–phenolic networks in nanomedicine: a review, *Biomater. Sci.*, 2022, **10**(20), 5786–5808.
199 J. Chen, *et al.*, Metal-phenolic networks as broad-spectrum antioxidant coatings for hemoglobin nanoparticles working as oxygen carriers, *Chem. Mater.*, 2022, **34**(20), 9200–9211.
200 C. L. Ventola, Progress in nanomedicine: approved and investigational nanodrugs, *Pharm. Ther.*, 2017, **42**(12), 742.
201 S. Soares, *et al.*, Nanomedicine: principles, properties, and regulatory issues, *Front. Chem.*, 2018, **6**, 360.
202 G. Lin, *et al.*, Designing metal–phenolic networks in biomedicine, *Appl. Mater. Today*, 2025, **45**, 102822.
203 Y. Xiao, *et al.*, Mechanochemical synthesis of cocrystal: From mechanism to application, *Cryst. Growth Des.*, 2023, **23**(6), 4680–4700.
204 N. Schultheiss and A. Newman, Pharmaceutical cocrystals and their physicochemical properties, *Cryst. Growth Des.*, 2009, **9**(6), 2950–2967.
205 A. Chettri, *et al.*, Pharmaceutical co-crystals: A green way to enhance drug stability and solubility for improved therapeutic efficacy, *J. Pharm. Pharmacol.*, 2024, **76**(1), 1–12.
206 A. Delori, T. Friščić and W. Jones, The role of mechanochemistry and supramolecular design in the development of pharmaceutical materials, *CrystEngComm*, 2012, **14**(7), 2350–2362.
207 Z. Wu, T. Cheng and Z. L. Wang, Self-powered sensors and systems based on nanogenerators, *Sensors*, 2020, **20**(10), 2925.
208 D. Zhang, *et al.*, Diversiform gas sensors based on two-dimensional nanomaterials, *Nano Res.*, 2023, **16**(10), 11959–11991.
209 H. Yang, *et al.*, Utilization of sea sand for preparation of high-performance CoAl2O4 composite pigments via a cleaner mechanochemistry route, *ACS Sustain. Chem. Eng.*, 2022, **10**(29), 9553–9564.
210 S. Sarfudeen, *et al.*, A Novel Mechano-Synthesized Zeolitic Tetrazolate Framework for a High-Performance Triboelectric Nanogenerator and Self-Powered Selective Neurochemical Detection, *ACS Appl. Mater. Interfaces*, 2024, **16**(19), 24851–24862.
211 Y. Qin, *et al.*, Interstitial/substitutional Se doping in nanosheet heterostructures for sensing NH3: Experimental and theoretical study, *ACS Appl. Nano Mater.*, 2023, **6**(20), 19290–19299.
212 Y. Hidalgo-Rosa, *et al.*, Expanding the knowledge of the selective-sensing mechanism of nitro compounds by luminescent terbium metal–organic frameworks through multiconfigurational ab initio calculations, *J. Phys. Chem. A*, 2022, **126**(39), 7040–7050.
213 V. Šepelák, *et al.*, Mechanochemical reactions and syntheses of oxides, *Chem. Soc. Rev.*, 2013, **42**(18), 7507–7520.
214 M. Sopicka-Lizer, *High-energy Ball Milling: Mechanochemical Processing of Nanopowders*, Elsevier, 2010.
215 A. S. Burange, Z. A. Alothman and R. Luque, Mechanochemical design of nanomaterials for catalytic applications with a benign-by-design focus, *Nanotechnol. Rev.*, 2023, **12**(1), 20230172.
216 Y. Nailwal, A. Rapid, *et al.*, Sustainable, One-step Mechanochemical Strategy for Synthesizing Gold Nanoparticle-Doped Covalent Organic Frameworks, *Chem.–Eur. J.*, 2025, **31**(22), e202500339.
217 J. E. Ogbezode, *et al.*, A narrative review of the synthesis, characterization, and applications of iron oxide nanoparticles, *Discover Nano*, 2023, **18**(1), 125.
218 V. Chaudhary, *et al.*, Mechanochemical synthesis of iron and cobalt magnetic metal nanoparticles and iron/calcium oxide and cobalt/calcium oxide nanocomposites, *ChemistryOpen*, 2018, **7**(8), 590–598.

219 O. Y. Posudievsky, *et al.*, Facile mechanochemical preparation of nitrogen and fluorine co-doped graphene and its electrocatalytic performance, *Carbon*, 2019, **152**, 274–283.
220 T. Tsuzuki, Commercial scale production of inorganic nanoparticles, *Int. J. Nanotechnol.*, 2009, **6**(5–6), 567–578.
221 A. Ali, *et al.*, Synthesis, characterization, applications, and challenges of iron oxide nanoparticles, *Nanotechnol. Sci. Appl.*, 2016, 49–67.
222 J. De Carvalho, *et al.*, Synthesis of magnetite nanoparticles by high energy ball milling, *Appl. Surf. Sci.*, 2013, **275**, 84–87.
223 S. Wu, T. Wang and H. Xu, Regulating heterogeneous catalysis of gold nanoparticles with polymer mechanochemistry, *ACS Macro Lett.*, 2020, **9**(9), 1192–1197.
224 A. Drmota, *et al.*, Microemulsion method for synthesis of magnetic oxide nanoparticles, *Microemulsions—An Introduction to Properties and Applications*, ed. Najjar, R., 2012, pp. 191–214.
225 I. Mitar, *et al.*, Rapid microwave method for synthesis of iron oxide particles under specific conditions, *Crystals*, 2021, **11**(4), 383.
226 M. J. Rivera-Chaverra, *et al.*, Synthesis of oxide iron nanoparticles using laser ablation for possible hyperthermia applications, *Nanomaterials*, 2020, **10**(11), 2099.
227 S. Pagola, Outstanding advantages, current drawbacks, and significant recent developments in mechanochemistry: A perspective view, *Crystals*, 2023, **13**(1), 124.
228 R. Luque, *et al.*, Evaluation of biomass-derived stabilising agents for colloidal silver nanoparticles via nanoparticle tracking analysis (NTA), *RSC Adv.*, 2013, **3**(19), 7119–7123.
229 Z. Shalabayev, *et al.*, Sulfur-mediated mechanochemical synthesis of spherical and needle-like copper sulfide nanocrystals with antibacterial activity, *ACS Sustain. Chem. Eng.*, 2019, **7**(15), 12897–12909.
230 T. Iwasaki, *et al.*, Synthesis of titanosilicate TS-1 crystals via mechanochemical route using low cost materials, *Microporous Mesoporous Mater.*, 2012, **150**, 1–6.
231 S. L. Tang, R. L. Smith and M. Poliakoff, Principles of green chemistry: PRODUCTIVELY, *Green Chem.*, 2005, **7**(11), 761–762.
232 P. F. de Oliveira, *et al.*, A mechano-colloidal approach for the controlled synthesis of metal nanoparticles, *Chem. Commun.*, 2019, **55**(95), 14267–14270.
233 Y. Xia, X. Xia and H.-C. Peng, Shape-controlled synthesis of colloidal metal nanocrystals: thermodynamic versus kinetic products, *J. Am. Chem. Soc.*, 2015, **137**(25), 7947–7966.
234 M. Klimakow, *et al.*, Mechanochemical synthesis of metal–organic frameworks: a fast and facile approach toward quantitative yields and high specific surface areas, *Chem. Mater.*, 2010, **22**(18), 5216–5221.
235 J. Shen and R. Blachnik, Mechanochemical syntheses of antimony selenide, tin selenides and two tin antimony selenides, *Thermochim. Acta*, 2003, **399**(1–2), 245–246.
236 Y. X. Shi, *et al.*, The first synthesis of the sterically encumbered adamantoid phosphazane P4 (NtBu) 6: enabled by mechanochemistry, *Angew. Chem.*, 2016, **128**(41), 12928–12932.
237 M. J. Muñoz-Batista, *et al.*, *Mechanochemistry: Toward Sustainable Design of Advanced Nanomaterials for Electrochemical Energy Storage and Catalytic Applications*, ACS Publications, 2018.
238 A. M. Belenguer, *et al.*, Solid-state dynamic combinatorial chemistry: reversibility and thermodynamic product selection in covalent mechanosynthesis, *Chem. Sci.*, 2011, **2**(4), 696–700.
239 S. Arfelis, *et al.*, Linking mechanochemistry with the green chemistry principles, *Heliyon*, 2024, **10**(14), e34655.
240 T. Friščić, *et al.*, Highlights from Faraday discussion 170: Challenges and opportunities of modern mechanochemistry, Montreal, Canada, 2014, *Chem. Commun.*, 2015, **51**(29), 6248–6256.
241 H. Mio, J. Kano and F. Saito, Scale-up method of planetary ball mill, *Chem. Eng. Sci.*, 2004, **59**(24), 5909–5916.
242 R. A. Buyanov, V. V. Molchanov and V. V. Boldyrev, Mechanochemical activation as a tool of increasing catalytic activity, *Catal. Today*, 2009, **144**(3–4), 212–218.
243 P. Y. Butyagin, Kinetics and nature of mechanochemical reactions, *Russ. Chem. Rev.*, 1971, **40**(11), 901.